GREEN SYNTHESIS OF IRON NANOPARTICLES (FeNPs) USING PLANT EXTRACTS AND THEIR APPLICATION IN THE DEGRADATION OF A VAT DYE

An MPhil thesis presented to the Department of Chemistry, University of Ghana

By

Peter Osei Ohemeng

(10406305)

In fulfilment of the requirement for the award of

Master of Philosophy

In

Chemistry

July 2019

Declaration

This thesis is a summary of the results of research work carried out by Peter Osei Ohemeng at the Department of Chemistry, University of Ghana, Legon under the supervision of Dr. Enock Dankyi (University of Ghana) and Dr. Vitus A. Apalangya (University of Ghana).

……………………………………… 20/06/2020 ………………………………

Peter Osei Ohemeng (Student) Date

……………………………………… 20/06/2020 ………………………………

Dr. Enock Dankyi (Supervisor) Date

……………………………… 20/06/2020 ……………………………

Dr. Vitus Apalangya (Supervisor) Date

Acknowledgement

I wish to express my profound gratitude to my supervisors who have helped make this work a reality. I am very grateful to my principal supervisor, in the person of Dr. Enock Dankyi for his immense support and contribution throughout my spell at the University of Ghana as a student. To Dr. Vitus A. Apalangya, my co-supervisor, I appreciate the love you showed me and my research work as well as the huge wealth of experience coupled with timely advice which facilitated the successful completion of this work.

I am also grateful to the senior members at the Department of Chemistry, University of Ghana whose rich contributions to this work by way of various seminar presentations have made it a successful one.

To my family, I say thank you for the continuous support and encouragement especially providing for my welfare as well as other contingencies.

Finally, I give the glory of this work to the Almighty God for His grace and strength that equipped me to complete this program.

Abstract

The growing concern for environmental sustainability calls for the adoption of 'greener' techniques for remediation purposes. The application of green synthesized iron nanoparticles (FeNPs) provides a promising route in this context. This thesis reports a facile room-temperature synthesis of stable iron nanoparticles utilizing aqueous extract of peels of *Musa sp.* (Plantain) and *Tetrapleura sp*. ('Prekese'). The extracts served as both reductants and capping agents owing to the myriad of polyphenolic compounds present. Synthesized nanoparticles were confirmed through visual inspection of colour changes and by the use of spectroscopic and microscopic techniques. Microstructurally, the synthesized iron nanomaterials using *Tetrapleura tetraptera* were non-discrete particles whereas the plantain (*Musa sp*.) mediated synthesized iron nanoparticles were uniformly shaped with approximate diameter within 80 nm and 100 nm range. Based on ultraviolet-visible (UV-Vis) data, prepared iron nanomaterials showed a maximum plasmon resonance absorbance at 300 nm, typical of nanoscale iron. Fourier transform infrared spectroscopy (FTIR) analysis indicated the presence of various functional groups, particularly hydroxyl, present in the extracts, which may be responsible for capping of nanoparticles.

The synthesized iron nanomaterials exhibited good efficiency in the degradation of Vat orange dye. The degradation process was highly dependent on contact time, pH, temperature, initial adsorbate concentration, and adsorbent dose. The sorption equilibrium of the dye on the nanoparticles was reached within 240 min of subjecting the aqueous solution of dye to the synthesized nanoparticles and was best explained by the Freundlich adsorption model.

The results from this study illustrate that biosynthesized iron nanomaterials offer a cost-effective, environmentally friendly and efficient means of remediation of dye-contaminated industrial effluents.

Table of Contents

Structure of Thesis

The entire thesis has been outlined in five chapters. The first two chapters give a general introduction as well as the relevant literature to the thesis. Chapters three and four describe the various experiments carried out and the obtained results in details. The last chapter presents the general conclusions and perspectives of the study. The primary intent is to present these findings as manuscripts for submission to international peer-reviewed journals. In summary:

Chapter 1 gives a general introduction to the thesis, describing the background of the study, stating the problem and outlining the aim and objectives of the study.

Chapter 2 captures the relevant literature of the topics understudy.

Chapter 3 focuses on the green synthesis and characterization of iron nanoparticles (FeNPs). The chapter also gives a brief introduction to the experiment, describes the detailed experimental work carried out and subsequently provides discussions and conclusions based on the results obtained.

Chapter 4 presents results on how the catalytic ability of the FeNPs are explored to degrade some locally available dyes (Vat orange dye). Similarly, the chapter provides a brief introduction to the experiment, clearly explains the experimental work carried out and subsequently outlines discussions and conclusions based on the results obtained.

Chapter 5 gives the general conclusions based on results as well as perspectives of the study.

CHAPTER ONE

1.0. General Introduction

1.1. Background

The increase in industrialization and other anthropogenic activities have become a huge source of pollution in aquatic and terrestrial environments in most countries. In the Sub-Saharan African region, while industrialization is generally low, the general lack of environmental awareness and the lack of (strict) adherence to regulations have contributed to massive pollution of water bodies over time. This has often resulted in the discharge of large amounts of untreated or inadequately treated effluents containing toxic substances including metals, organic and inorganic waste into the environment.

Untreated effluents pose major environmental challenges. For instance, the textile industry employs several kinds of dyes and ultimately exude large amounts of colourful effluents into water bodies as a result of the poor, uptake of these dyes by fabrics. The untreated dye effluents may have adverse effects on aquatic life, including loss of photosynthetic function in plant, low light penetration and loss of oxygen (Holkar *et al.*, 2016).

Recently, nanotechnology has emerged as an important technique for environmental remediation. While the technology is burgeoning, this area of research has evinced the possibility to be applied in numerous fields including electronics, optics, microbiology, biotechnology and broad fields of engineering and materials science. Nanoparticles possess a number of unique characteristics including reduced size, uniform size distribution, larger surface area, photocatalytic activity and biocompatibility (Bishnoi *et al.*, 2018), making them suitable for use as agents for environmental remediation.

Although there are a number of nanoparticles derived from several sources with good environmental remediation properties, iron nanoparticles are preferred due to their cost-effectiveness, natural abundance and good recoverability (Carroll *et al.*, 2013). Currently, there have been several advances in nanotechnology with regard to wastewater treatment and remediation which has resulted in the growth of new nanoparticles for the extrication of contaminants such as nitrates, chlorides and heavy metals (Giraldo *et al.*, 2013; Kassaee *et al.*, 2011; Saif *et al.*, 2016). Iron nanoparticles have remained effective in remediating several synthetic and non-synthetic pollutants in the environment (Calderon & Fullana, 2015). This could be ascribed to the intrinsic properties of FeNPs viz: increased reactivity for immobilization of pollutants and high kinetic energy in porous media (aquifers, soil) (Calderon & Fullana, 2015).

The catalytic and reductive characteristics of iron nanoparticles ($E_o = 0.44V$) present them as good environmental remediation agents (Zhao *et al.*, 2016). In this regard, they have been largely employed in the reduction of organic dyes (Sangami & Manu, 2017) and the adsorption of heavy metals such as chromium (Jin *et al.*, 2018). However, the activity of iron nanomaterials has been reported to be influenced by geochemical processes, passivation, and agglomeration (Chien et al., 2005; Liu & Lowry, 2006; Johnson *et al.*, 2013; Zhao *et al.*, 2016). The magnetic property of FeNPs relies greatly on their synthetic approach, reaction time, use of reducing agent, use of surfactant and temperature (Nabiyouni *et al.*, 2015). This intrinsic property of FeNPs makes them coagulate rapidly, causing an integral decline in reactivity (Phenrat *et al.*, 2006; Tourinho *et al.*, 2012). In view of this, a number of stabilizers have been applied to these nanomaterials to ensure that, they do not develop into micron-sized particles.

The size and morphology of iron nanomaterials greatly affect their performance (An *et al.*, 2012). Hence, various synthetic approaches geared towards size and morphology controls have been utilized. These include top-down, chemical bottom-up and green bottom-up methods (Amendola *et al*., 2011; Ksv, 2017; Fu *et al.*, 2018; Zhao *et al.*, 2016). However, the latter is highly preferred due to its simplicity, cost-effectiveness and environmental benignity compared to the sophisticated and expensive top-down methods.

Chemical synthetic techniques have been reportedly used in the synthesis of inorganic nanoparticles with considerable success, although high cost and scalability concerns have arisen (Shah *et al.*, 2018; Xiao-Li Li 1, 2018). The mere controls required in achieving the desired surface morphology in some chemical synthesis procedures increase the cost of scaling up nanoparticle production. Also, the chemical reagents used as reductants such as sodium hydroxide (Kostyukova & Chung, 2016), hydrazine (Druzhinina *et al.*, 2011), N,N-dimethylformamide (Azuma *et al.*, 2018) and some organic stabilizers (thiol organic groups) may be toxic and hazardous to the environment.

As a result of these concerns, green synthetic techniques are rapidly emerging as sustainable alternatives to conventional methods (Gautam *et al.*, 2018; Devatha *et al*., 2016; Machado et al., 2015). Biosynthesis of iron nanoparticles (FeNPs) using enzymes, microorganisms or extracts of some plant materials have proven to be environmentally benign options to chemical synthesis methods (Narayanan & Sakthivel, 2010). Synthesis of iron nanomaterials using plant materials has several advantages over other biological processes in terms of scalability, ease, and cost of preparation and preservation of materials. For instance, plant extract mediated synthesis avoids the use of sophisticated and expensive procedures of preserving cell cultures and is highly biocompatible. Generally, the use of plant material in preparing iron nanomaterials is gaining widespread attention in recent times because plant extracts contain a myriad of poly-phenolic compounds that offer researchers an alternative cost-effective and non-hazardous, simultaneous reduction and stabilization during the synthesis. Several extracts from plant parts have been evaluated and employed in the synthesis of iron nanomaterials. These include leaves (Cao *et al.*, 2016; Jin *et al.*, 2018; T. Wang *et al.*, 2014; Z. Wang *et al.*, 2014), buds and seeds (Afsheen *et al.*, 2018), roots (Radini *et al.*, 2018) and other plant parts (Murgueitio & Debut, 2016). More importantly, the plants used for the synthesis should not compete within the food chain where they are used as food.

The bulk composition, surface chemistry and particle size among other properties of nanomaterials have huge impacts on the efficacy of their performance. Reports suggest that, these characteristics are time-dependent because of the high reactivity of nanomaterials (Chekli *et al.*, 2016) hence, optimization of synthesis to ensure stability is often needed. Several analytical tools such as transmission electron microscopy (TEM), scanning electron microscopy (SEM) and X-ray diffraction (XRD) have been employed to characterize and optimize FeNPs particles.

In this work, an environmentally benign preparation of FeNPs particles utilizing the extracts of *Musa sp*. (plantain) and *Tetrapluera sp*. (locally referred to as 'Prekese') is described. The study also reports its characterization and application in the remediation of Vat orange dye.

1.2. Problem statement

Increasingly, anthropogenic activities raise alarming concerns about the quality of the environment. While the products from these activities may be important to humans, the potential harm to living organisms and the environment from waste and by-products from these activities remains a concern. The need for more effective and efficient techniques in addressing this challenge is an area that continues to attract much attention among scientists. In this regard, nanotechnology offers great promise in the environmental remediation of contaminants. In particular, iron nanoparticles (FeNPs) have been employed as an efficient environmental remediating agent for a large number of pollutants in diverse environmental media. The ability of FeNPs to remediate the environment has been ascribed to their inherent small size, which translates into larger specific surface area, and a higher density of reactive surface sites, making them highly reactive. The challenge, however, is the application of environmentally benign methods to produce FeNPs which are stable and highly reactive.

Among other aims, this study sought to produce FeNPs using a simple, fast and eco-friendly approach and to explore the catalytic ability of the produced FeNPs on the degradation of a locally used dye.

1.3. General research objectives

1.3.1. Aim

The primary aim of this study is to prepare iron nanomaterials via a green synthesis approach using locally available plant materials and to apply the nanomaterials in the degradation of Vat orange dye.

1.3.2. Specific Objectives

The specific objectives of the present study are:

- To synthesize and fully characterize iron nanoparticles (FeNPs).
- Apply the ‘as prepared’ nanomaterials in the degradation of locally used dyes.

- Examine the impact of pH among other factors on the adsorption of a pollutant dye by iron nanoparticles (FeNPs).

CHAPTER TWO

2.0. Literature review

2.1. Evolution of FeNPs-based technology and production of stable FeNPs.

2.1.1 A concise history on the origination of FeNPs-based remediation technology

In the past years, the use of various forms of iron in soil and groundwater clean-up has witnessed considerable improvement in technology from iron filings to stabilized FeNPs (Zhao *et al.*, 2016). The development observed in FeNPs-controlled clean-up technique can be divided into the following:

1) Preparation and characterization of essential bare ironparticles, which are predominantly aggregates with certain components in the nanoscale region.

2) Reduction in chlorinated solvent dechlorination e.g., tetrachloroethylene / trichloroethylene and polychlorinate biphenyls (TCE & PCBs).

3) Synthesis, characterization and assessment of the behavior of stable FeNPs for reduction of dechlorination and reduction of redox-active immobilization. and

4) Study of the fate, transport and toxicity of both stabilized and non-stabilized FeNPs.

As existed before now, bare iron nanoparticles had been prepared by reducing an Fe^{2+}/Fe^{3+} salt with a strong reductant (borohydride) in the aqueous phase. This method was pioneered by (Schlesinger *et al.*, 1953) when they reduced some transition metals, which included Fe^{2+} with borohydride to enhance the production of hydrogen. In 1962, it was noticed that borohydride was used to reduce a number of platinum metals which included Fe^{2+} to their elemental state (Brown *et al.*, 1962). However, the basis of chemistry on how this happens was unknown until 1990 and 1995 when the size of synthesized iron powder was first described by the term “nanoscale Fe powder” (Corias *et al.*, 1990; Glavee *et al.*, 1995).

Senzaki (1991) and Senzaki & Kumangai (1988a,1998b) concluded in their study that, powdered iron successfully reduced chlorine-based organic substances in wastewater. Prior to that, the maiden environmental application of FeNPs had been published by Gould (1982) where he studied the rate of reduction of hexavalent chromium by metallic iron wire. Granular zero-valent iron nanoparticles saw their first field application when they were employed in a permeable reactive barrier (PRB) to remove TCE and PCE in groundwater (Guan *et al*., 2015; O'Hannesin and Gillham, 1993). The efficacy of the technique used caused a rapid increase in the employment of zero-valent iron nanoparticles in PRBs.

The general idea of *in situ* dechlorination by FeNPs in the subsurface was conceptualized firstly by Wang and Zhang (1997), where they made several postulates of which one suggests that FeNPs may be introduced directly into contaminated soil or groundwater to enhance *in situ* remediation. In their study, they demonstrated the potency of synthetic, bare zero-state iron nanoparticles on reductive dechlorination and concluded that manufactured FeNPs is more reactive than commercially available powder iron. In the quest to know the effect a metal catalyst may have on the behaviour of synthesized FeNPs, Zhang *et al*., (1998), suggested that addition of limiting amount of palladium (Pd) metal may boost the surface-area-normalized rate constant manifold. This improved remediation technique enticed many researchers considering the abundance of chlorinated hydrocarbons in soils.

However, earlier works focused much on aqueous media and hence failed to adequately include further essential information with connections to soil remediation, including soil deliverability and particle agglomeration. Further studies therefore focussed on soil transportability and particle stabilization (Schrick *et al*., 2004; He and Zhao, 2005; He *et al*., 2007).

2.1.1. Preparation of non-stablized FeNPs

Iron nanoparticles (FeNPs) were mainly generated using either of these three main techniques:

1) Top-down processes comprising high-energy surface friction of micro-sized iron particles.

2) Bottom-up methods, that is the reduction of Fe^{2+}/Fe^{3+} in the aqueous phase.

3) Reduction of iron oxides in the gaseous phase through scalable approaches such as hydrogen gas. Ball-milling of commercial iron powder for about half an hour successfully yielded iron aggregates of specific surface area. A more reactive FeNPs with a much-improved surface area and smaller size was obtained after 8h of further milling (Li *et al*., 2009). Amidst these advantages of less energy and less time associated with this method, the produced FeNPs showed comparably good performance with those manufactured via conventional aqueous reduction using borohydride. However, this method could not stand the test of time as the particles rapidly coagulate in water into micron-sized particles raising negative concerns of particles deliverability in soil.

In general, bottom-up methods remain the most widely reported technique of FeNPs production. This involves utilizing $NaBH_4$ to reduce ferrous or ferric ions under inert atmosphere (He and Zhao, 2005, 2007; Wang and Zhang, 1997). The following equations explain the process:

$$Fe(H_2O)_6^{3+} + 3BH_4^- + 3H_2O \rightarrow Fe^0_{(s)} + 3B(OH)_3 + 10.5H_{2\,(g)}. \qquad (1)$$

$$2Fe^{2+} + BH_4^- + 4H_2O \rightarrow 2Fe^0_{(s)} + B(OH)_4^- + 4H^+ + 2H_{2\,(g)} \qquad (2)$$

However, this wet chemical synthesis method of FeNPs is rarely used nowadays because of the high cost and toxic nature of the sodium borohydride used for the reduction.

In an attempt to resort to a cost-effective, “greener” and a more eco-friendly way of preparing FeNPs, some organic reductants and stabilizers have been utilized. For instance, stabilized FeNPs particles have been prepared by the reductive action of polyphenolic compounds from leaves of

Eucalyptus on an iron precursor (Weng *et al.*, 2016). The form in which these FeNPs appeared (size and morphology) was dependent on the concentration of the extract. This presupposed that, injecting organic reducing agents into a medium with significant traces of ferric and ferrous ions may yield FeNPs. Nonetheless, the yield of FeNPs would be dependent on the concentration of the ferric or ferrous ions in conjunction with other factors.

2.1.2. Production of capped or stabilized FeNPs

Metal nanoparticles agglomeration is a significant challenge for researchers in nanoscience. Agglomeration in nanoparticles is a thermodynamically feasible process that tends to cause individual particles to cluster together to form larger particles depriving the nanoparticles of their expected behaviour in subsurface. This process occurs either by:

1) Ostwald ripening (that is, particles lower than the critical size are dissolved and taken by bigger particles during particle growth and formation).

2) Arrested precipitation (precipitation enhanced by nucleation centre formation).

3) Direct inter-particle interactions. (He and Zhao, 2005, 2007; Laurent *et al.*, 2008; Sun and Zeng, 2002).

Several inter-particle forces namely, magnetic dipolar interactions, van der Waal's forces and electric dipolar interactions may contribute to particle agglomeration. Agglomeration of particles reduces particle deliverability in soil and hence diminishes particle reactivity by reducing the specific surface area. In this regard, the ability to control the inter-particle interactions, which eventually leads to particle growth, as well as depriving particle surfaces of nimble reactions by the media directly corresponds to particle stabilization.

Several stabilization techniques have been investigated and adopted to help improve the dispersibility and stability of FeNPs. In general, the production of stable iron nanoparticles can be achieved either by modifying the FeNPs surfaces or separating the nanoparticles by creating a network. In the network stabilization fashion, higher doses of stabilizers are added to promote the creation of a network via polymer twisting and hydrogen bonding (Comba *et al*., 2009) which in effect hampers particle agglomeration. The network stabilization occurs in two folds:

1) the stabilizer is attached onto the FeNPs and this incorporates the FeNPs within the gel structure or 2) a non-adsorbing stabilizer is added to generate a network around FeNPs particles which causes the nanoparticles to segregate. When this happens, the rate of collisions between the nanoparticles declines by virtue of the rigidity of the stabilizer matrix or the network where the nanoparticles are stacked (Tosco *et al*., 2014). In the surface modification stabilization method, repulsive forces such as: electrostatic repulsion and osmotic or electrosteric repulsion are enhanced through the attachment of stabilizers onto the FeNPs surface. This refrains the nanoparticles from developing into micron-sized particles (coagulation).

It has been established that the addition of stabilizers to FeNPs increases nanoparticle dispersion. This is realized through the underlisted processes:

1) electrostatic stabilization (establishment of Coulombic repulsion between stabilized particles as a result of adsorption of charged stabilizer molecules to the metal core).

2) steric stabilization (coating surfaces of the metal core with stabilizers in the form of polymers which will impede particle affinities via osmotic repulsive force, arising from overlap of stabilizer molecules).

3) electrosteric stabilization (through combined electrostatic and steric interactions).

4) network stabilization (or viscous stabilization).

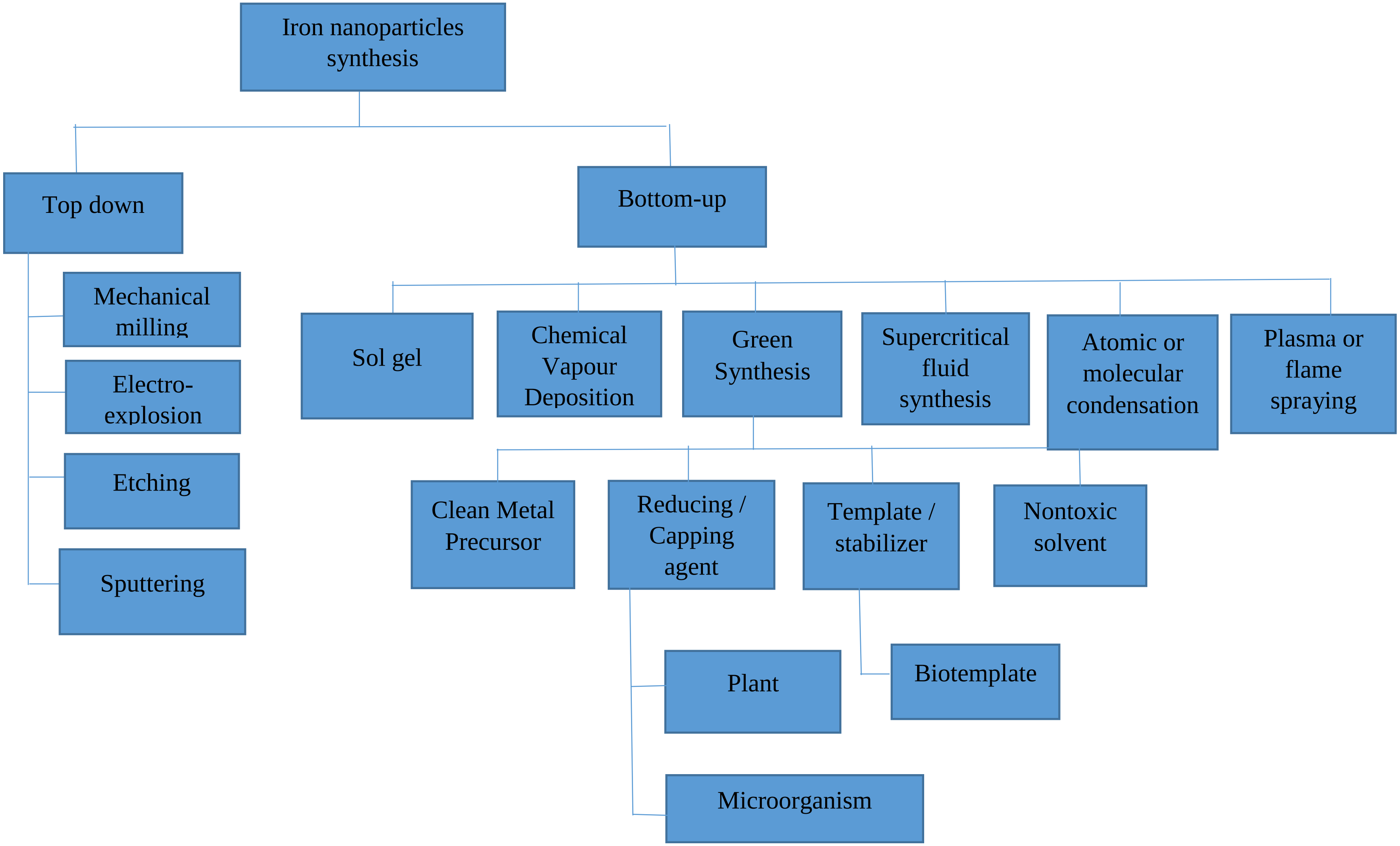

Figure 2.1. Various methods employed in the synthesis of iron nanomaterials. Adapted from (Genuino *et al.*, 2013)

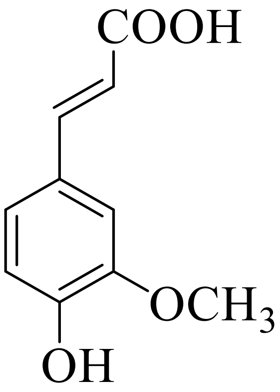

Fuluric acid

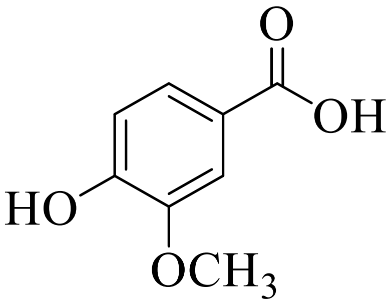

Vannilic acid

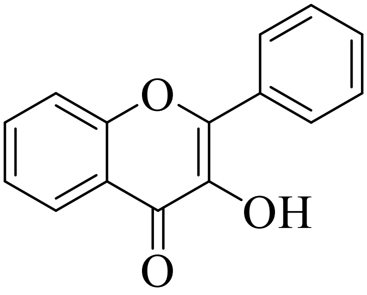

Flavanol

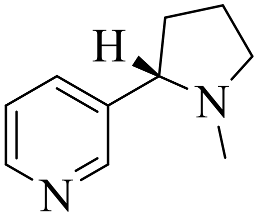

Alkaloid

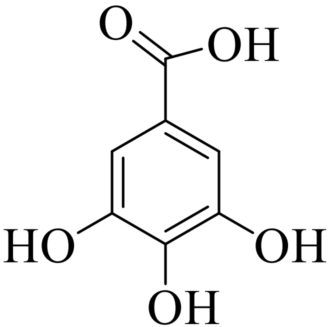

Tannin

Figure 2.2. Structures of some organic compounds present in plant extracts responsible for reducing and capping nanoparticles.

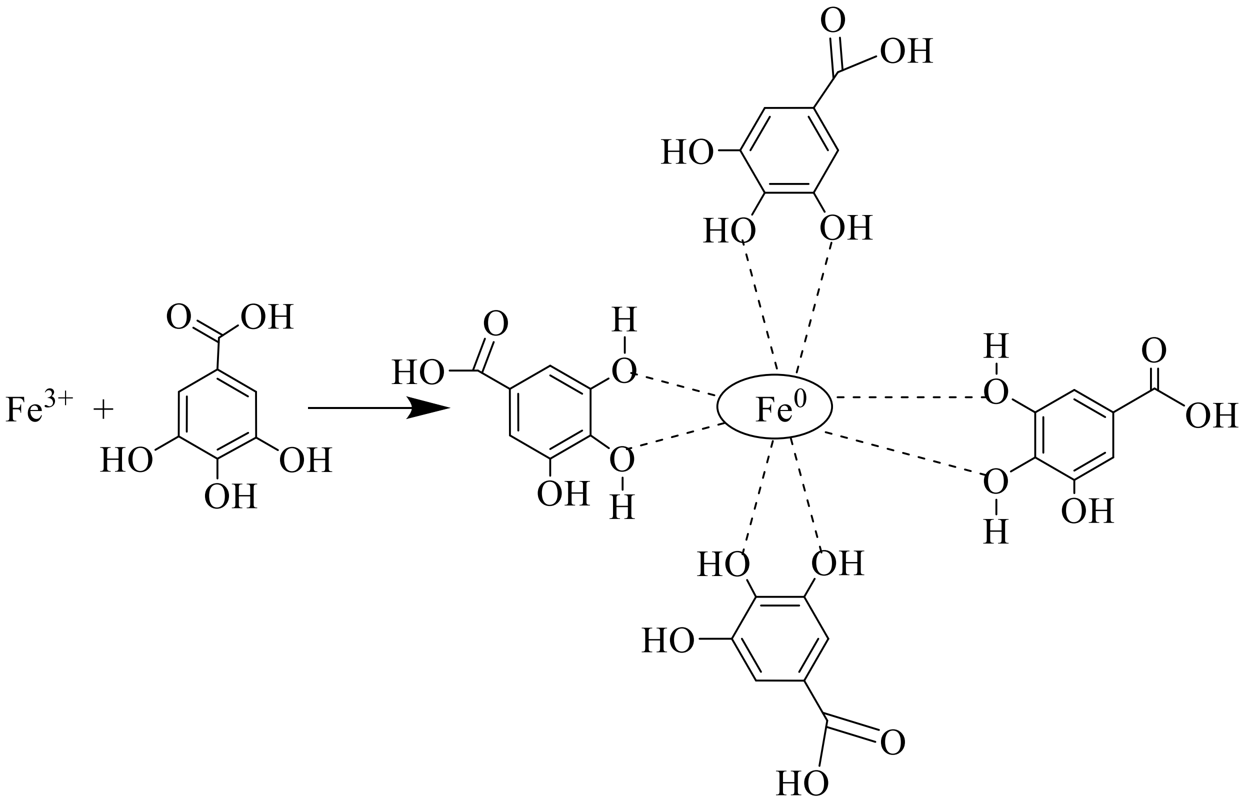

Figure 2.3. Proposed reduction and capping of iron by Tannin, a phytochemical present in plant extracts.

2.2. Properties of FeNPs

Iron nanoparticles (FeNPs) are iron-containing materials with dimensions of about 1 to 100 nm. Primarily, the structure of stable FeNPs is made up of an iron core, which is greatly clustered by several stabilizers.

Just like other nanomaterials, the general properties of FeNPs based on their structure and functionalities play a significant role in their application and reactivity. According to Kirsten *et al*. (2017), these properties are classified into three primary groups, namely:

1) "what they are" (characterization): chemical and physical characteristics in their structure, impurities, size and size distribution, shape, surface features (coating, chemistry, surface characterization), surface region and porosity.

2) "where they go" (fate): biological (toxicokinetics, bio-distribution) and environmental fate.

3) "what they do" (reactivity): physical hazards, biological reactivity, toxico-dynamics, photo-reactivity, etc.

In terms of their characterisation, most FeNPs appear as extremely small-sized, magnetic and charged species. Their relatively large surface area due to their reduced size makes them exhibit higher kinetic energy compared to their bulk counterparts. This enables them to have an uncontrollable fate, especially in the environment, as they can penetrate tiny media spaces. Compared to bulk iron, the reactivity of FeNPs is much pronounced. This explains why FeNPs have been utilized to execute different tasks in different fields. For example, FeNPs have successfully been applied for several environmental remediation purposes over the last decade because of their highly reactive nature.

2.3. Applications of well-capped FeNPs for environmental remediation

Despite the existence of widespread applications for stabilized FeNPs, applications have primarily been studied and investigated for environmental remediation. This is so because the rudiments of the activity of FeNPs are per their electron-donating properties. As expected, the excellent electron-donating prowess of FeNPs presents them as versatile remediation agents as they are sufficiently reactive in water (Socas-Rodríguez *et al.*, 2017). Over the last few years, several studies have revealed the efficacy of highly reactive and well capped FeNPs for the remediation of many pollutants including trichloroethene (TCE) and perchloroethene (PCE), nitrates, heavy metals and some organic dyes. Taking into perspective the transformation of organic contaminants by FeNPs as a remediation technique, the proposed removal processes involve: the FeNPs providing a surface for the chlorinated organics to adsorb onto and subsequently cleaving the carbon-halogen bonds (Weber 1996). In a study by Chen *et al*., (Chen *et al*., 2011) on aqueous degradation of azo dyes by FeNPs, the adsorption of dye molecules onto FeNPs surfaces and subsequent reduction through a free radical intermediate has been proposed as the mechanism for remediation. The FeNPs react with H_2O to generate hydrogen radicals which act on the azo bond (-N=N-), causing it to cleave. Below is an illustration of the removal mechanism of methyl orange dye from aqueous solution as proposed by Chen *et al*., (2011).

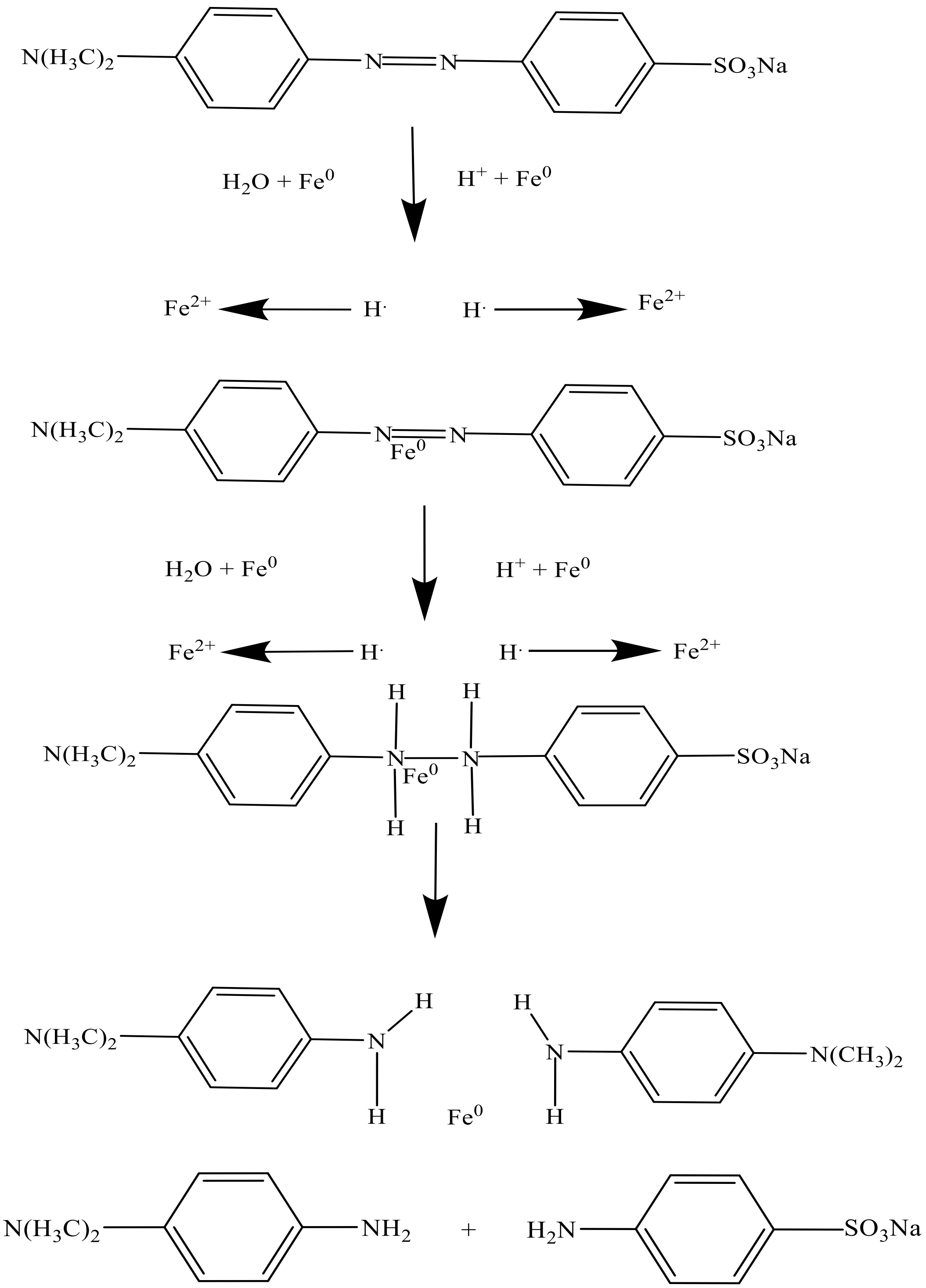

Scheme 1. Proposed removal mechanism of methylene blue dye from aqueous solution. The figure is redrawn from (Chen *et al.*, 2011).

Vat dyes are among the commonly used dyes in the textile industry. As such, their residues have become a major environmental pollutant in most locations where they are used. These dyes are brightly coloured and have a large presence of chromophores and auxochromes. Several forms of vat dyes with different colours are extensively used in dyeing cotton fabrics. The inherent stability of these dyes makes them less susceptible to bio-degradation and hence often requires other remediation pathways. In literature, iron nanomaterials have been successfully utilized as a catalytic agent in the reduction of Vat green 1 dye (Simin Arabi, 2012).

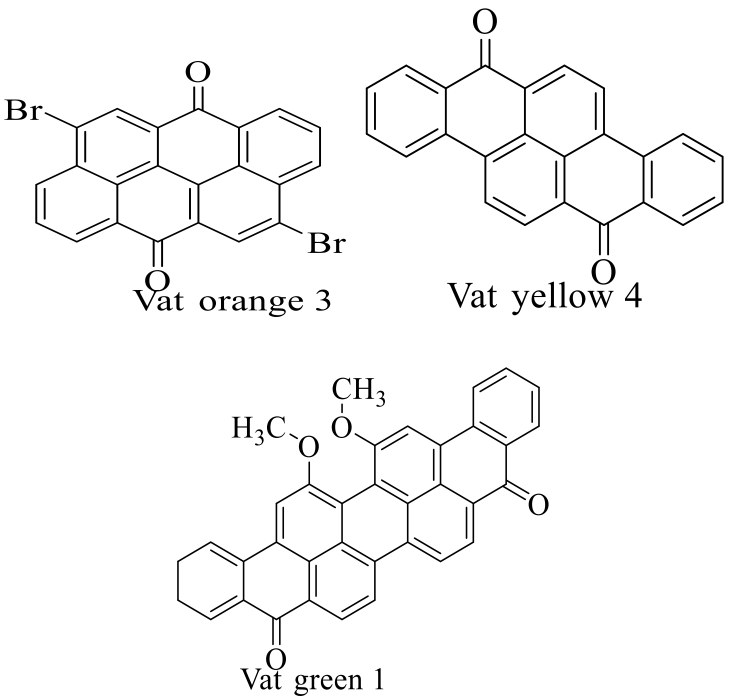

Vat orange 3 Vat yellow 4

Vat green 1

Figure 2.4. Examples of some locally used vat dyes

Stabilized FeNPs have been commonly examined for the immobilization of heavy metals together with other contaminants in the environment. The advantages of high reducing power and high deliverability of FeNPs in soil have seen them widely used for this purpose. High percentages of heavy metal removal by FeNPs have been recorded over the last few years. With reference to the removal mechanism, FeNPs double as surfaces and reductants (Jin *et al.*, 2018). Meanwhile, the immobilization mechanism of heavy metals by FeNPs proceeds through an initial formation of iron oxide (Xue *et al.*, 2018)

The iron oxide shell formed allows for sorption and surface complexation of metal ions which are required for the removal process (Xue *et al.*, 2018). Therefore, the immobilization of metals by FeNPs can be explained as follows:

$FeO^- + M^{2+} \rightarrow FeOM^+$

$FeOH + M^{2+} + H_2O \rightarrow FeOMOH + 2H^+$ where M is a metal.

2.3.1. Factors Influencing the performance of FeNPs

Many literature have illustrated the dependence of the performance or reactivity of FeNPs on several factors. Chief of which are stabilizers, pH, surface area, temperature and initial concentration (He *et al.*, 2009; Phenrat *et al.*, 2016; Senthil Kumar *et al.*, 2017). These factors and their effect on the activity of nanomaterials are discussed below:

2.3.1.1. Temperature

As established earlier, the removal mechanism of contaminants by FeNPs proceeds via an adsorption process. Adsorption is possible via physical (physisorption), chemical (chemisorption) or a combination of both depending on the extent of the process with change in temperature at constant pressure. Enthalpy change (ΔH^o), a thermodynamic quantity, serves as an indicator for observing the type of adsorption occurring in a particular system. Negative ΔH^o values indicate the loss of energy during adsorption; hence, heat energy used in adsorption becomes negative, indicating an exothermic process (Senthil *et al.*, 2017).

According to Weng *et al*., (2016), the rate of adsorption of contaminants onto FeNPs surfaces is enhanced at high temperatures with subsequent decline at low temperatures. However, contrary to the findings by Weng *et al.*, (2016), Senthil *et al.*, (2017) have reported higher removal efficiency of contaminants at lower temperatures due to improved adsorption rates at these temperatures leading to rapid mobility of contaminants from solution onto FeNPs surfaces. Per these findings, there is a decisive role played by temperature on the activity of FeNPs, although the exact effect may be different depending on the mechanism of action.

2.3.1.2. pH

pH is an essential parameter in the determination of the reactivity of FeNPs in an aqueous medium. He *et al.,* (2009) carried out FeNPs-based remediation of chlorine contaminated soil. Major findings from their study demonstrated that weak acidic conditions might favour the dechlorination process (He *et al.*, 2009). Further findings suggested that within a system of pH 5.5, the amount of H^+ available is enough to trigger the production of H_2 through iron corrosion. However, at a much lower pH of 3.6, the surface of FeNPs become covered by H_2, which inhibits the adsorption process hence reducing the dechlorination process. Generally, the solution pH influences the frequency of adsorbates adhering onto the adsorbent surface. Cr (VI) metal (which exist as anion species in aqueous solutions) thrives well under acidic condition as it is readily adsorbed onto the more positively charged FeNPs surface. In contrast, the removal of Cu (II) is enhanced at an increased pH. This is so because the FeNPs surface is sufficiently covered by H^+ ions at lower pHs which repel the positively charged Cu(II) ions hence thwarting the adsorption of the metal onto the adsorbent for reduction to occur (Weng *et al.,* 2016).

2.3.1.3. Surface area

Surface area remains one of the intrinsic parameters of FeNPs that impact greatly on their performance or reactivity. Bishnoi *et al.*, (2018), observed higher percentage degradation of dye when treated with iron nanoparticles indicating that iron nanoparticles may be better catalysts than other dye degradation agents. This phenomenon may be due to the large specific surface area of the iron nanoparticles (FeNPs). Increase in surface area correspondingly increases the frequency of active sites on the FeNPs surface; hence, escalating their propensity to be used as catalysts in many applications. Generally, the reactivity of FeNPs declines as specific surface area shrinks. This phenomenon was affirmed in a report by Crane *et al*.(2015), (Crane *et al.*, 2015) which showed a decrease in adsorption of some radionuclides onto FeNPs surface due to a reduction in surface area of the sorbent. However, large surface area contributes to FeNPs agglomeration resulting in a decrease in reactivity and particle movement. This makes the need for optimization of stability of nanoparticles prior to field application even more vital.

2.4. FeNPs Stabilization

Due to the inherent magnetic properties of FeNPs, particle conversion into micron-scale level is quite rapid. This, in effect, reduces particle mobility and deliverability in soil or water. To optimise the efficacy of FeNPs for environmental remediation, various stabilization methods have been examined and developed (He *et al.*, 2009). Several chemical substances, including enzymes and other organic compounds in plants have successfully been used to stabilize FeNPs. However, in recent years many researchers have relied on organic-based stabilizers, as chemical stabilizers are often of high cost and may pose some environmental concerns. The activity or performance of FeNPs is improved when the individual particles are well capped or stabilized. For example, (Shanker *et al.*, 2017) demonstrated excellent degradation efficiencies by organic stabilized iron nanoparticles (FeNPs) on polyaromatic hydrocarbons (PAHs). Also, well-capped iron nanomaterials were successfully used as a fenton-like catalyst to degrade ametryn; an organic dye in water (Sangami & Manu, 2017).

The good promise shown by FeNPs for in situ remediation per the scenarios above suggests that reactivity is much pronounced when particles are well stabilized.

2.5. Fate and Toxicity of FeNPs

While a number of studies have focussed on the general fate and toxicity of nanoparticles, there is a considerable gap in the literature on the fate and toxicity exclusive to the different oxidation states of iron nanoparticles (Kreyling *et al.*, 2006).

Generally, the geochemistry of a system (groundwater or soil) greatly affects the fate of FeNPs particles. The concentration of contaminants, process of preparation of FeNPs, FeNPs particle ageing, particle agglomeration among other properties remain as issues that continually affect the fate of FeNPs within groundwater and soil.

According to Zhao *et al.*, (2016), stabilized FeNPs must possess high mobility in order to penetrate a target medium for practical applications. However, it is expected that once the injection is made, external pressure is released and the delivered nanomaterials must remain immobile within a domain, where the particles themselves and stabilizers pose no or less environmental threat. Keane (2009), made a similar argument outlining that, the susceptibility of bare FeNPs to agglomeration provides no worry for practical applications in groundwater remediation (keane, 2009).

However, there is a slim line that separates the detrimental and advantageous fate of FeNPs. This is because, the much sought-after properties and reactions that may make the particles an efficient remediation agent remain the same for those that may increase the potential risk of FeNPs to human health or the environment. For instance, self-aggregated FeNPs potentially associate themselves with sediments or suspended solids via bioaccumulation and may pose a significant threat in post *in-situ* remediation (Karn *et al.*, 2009).

One of the numerous recommendations is to research into the design of analytical tools that could be used to identify and monitor nanoparticles in the environment.

Largely, there has been reduced concerns with respect to the toxicity of FeNPs. This is as a result of the existence of iron oxides, which primarily persists in groundwater as rust. Nonetheless, there are increasing concerns linked to the application of FeNPs for environmental remediation. These are largely due to the detrimental effects associated with the continuous accumulation of iron in the body. Accumulation of iron to large amounts in the body may lead to oxidative stress, DNA damage, lipid peroxidation and carcinogenesis (Ashamed, 2014). Iron toxicity is dependent on its capacity to control the production of hydroxyl radicals ($OH^{\cdot}$) from superoxides and peroxides. These highly reactive free radicals may affect antioxidant enzymatic activities leading to eventual damage of cell and tissue (Li *et al*., 2009) Potential risks involved in FeNPs applications on human, mammals and aquatic organisms have been extensively studied (Hristozov & Malsch, 2009; Khan, 2013). However, a great tool employed in these studies has always been the understanding of the routes of exposure of FeNPs to these organisms.

Several findings have established toxicity concerns of FeNPs in mammalian nerve cell, adult fish, viruses and bacteria (keane, 2009; Khan, 2013).

Despite the potential negative implications, FeNPs offer an important eco-friendly alternative to environmental remediation. However, toxicity and useful concerns of FeNPs should be considered before their application.

CHAPTER THREE

3.0. Green synthesis and characterization of iron nanoparticles (FeNPs).

3.1. Introduction to Chapter Three

The adoption of greener environmental processes has been on the increase in response to concerns about the quality and sustainability of the environment. This is reflected in the numerous publications on green chemistry and green processes within the past years. These green approaches have often involved the use of techniques including microwave-assisted, ultrasonic fields, lithography and laser ablation (Suh *et al.*, 2012; Wang *et al.*, 2012; G.Q. Zhang *et al.*, 2007; R. Zhang *et al.*, 2014). These techniques have been utilized in the preparation of nanoparticles. However, they are of high cost and may involve the use of harsh chemicals. In this regard, current synthetic approaches are focused on developing methods which are relatively cheap and have less or no impact on the quality of the environment (Narayanan & Sakthivel, 2010).

Syntheses of nanoparticles using biological materials such as plant extracts, vitamins, sugars, microorganisms and enzymes have emerged in recent years and widely adopted by researchers. The processes for preparing nanoparticles utilizing biological reagents as both reductants and stabilizers have been shown to be an attractive option in nanotechnology (Kharissova *et al.*, 2013). In view of this, many metal nanomaterials, including iron nanoparticles (FeNPs), have been produced utilizing this technique. Green synthesis of nanomaterials provides many advantages compared to other methods as simple, eco-friendly and cost-effective technique. Among all the naturally occurring reagents employed in the green synthesis of nanomaterials, plant materials appear as the most suitable due to ease of scalability and biocompatibility of nanoparticles produced.

Bare iron nanomaterials have traditionally been synthesized using three main techniques, including top-down techniques, bottom-up techniques and gas-phase reduction of iron oxides to zero-valent iron (Zhao *et al.*, 2016). The bottom-up method involving reduction of iron precursor with sodium borohydride in an aqueous medium is often used to prepare FeNPs. However, the corrosive, toxic and flammable $NaBH_4$ generates flammable hydrogen in the process which is hazardous and also restricts large-scale productions of FeNPs (Zhao *et al.*, 2016).

Currently, iron nanomaterials have been prepared by green approaches where plant-based materials are employed as both reducing and capping agents.

Extracts of different plant parts have been reported in the literature to be used for the syntheses of iron nanomaterials. The presence of a plethora of poly-phenolic compounds in the plant extracts affords them the ability to cap the individual nanoparticles hence stabilizing them.

In this context, some locally available plant biomass comprising *Tetrapleura sp.* (locally referred to as 'Prekese' in Ghana) and Plantain peels (*Musa sp.*) extract were employed to biosynthesize the iron nanomaterials.

Tetrapluera sp., a flowering plant which belongs to the family *Fabaceae* is mostly found in West African countries. It has been reported to contain several phytochemicals which include, tannins, flavonoids and starch. These phytochemicals have the ability to reduce iron salts and are able to adequately cap metal nanoparticles because of their numerous hydroxyl groups which confer on them higher reduction potential and chelating powers.

Plantain, on the other hand, is cultivated in large quantities in tropical areas. It belongs to the family *Musaceae*. The peel of plantain has been reported to be rich in starch and protein (amino acid)

(Happi Emaga *et al.*, 2007). The starch content of the plantain peel may serve the dual purpose as the reducing and capping iron nanoparticles during their preparation.

Largely, the use of these plant materials does not compete with humans as a source of food for consumption. More importantly, iron nanomaterials of different sizes and morphology may behave differently in a contaminated environment. This, therefore, proposes the need to characterize nanomaterials prior to their applications.

Herein, the green preparation and characterization of FeNPs utilizing extracts of *Tetrapleura sp.* and *Musa sp.* is presented.

3.2. Materials and methods

3.2.1. Reagents and equipment

The following analytical grade reagents were used directly as obtained, thus without any further treatment throughout the work: ethanol (96%), Ferric chloride hexahydrate ($FeCl_3 \cdot 6H_2O$), glacial acetic acid, potassium ferrocyanide and sulfuric acid. 0.1 M portions of hydrochloric acid (HCl) and sodium hydroxide (NaOH) were prepared and used in this work.

Deionized water was used throughout the experimental work. The instruments employed in the study include a Perkin-Elmer FTIR spectrophotometer, a SHIMADZU UV-1800 UV-Vis spectrophotometer, transmission electron microscope (TEM) and a computer-controlled X-ray diffractometer.

3.2.2. Preparation of Extracts

3.2.2.1. Collection of Plant materials

Riped plantain (*Musa sp.)* and fruits of *Tetrapleura sp.*were obtained from a market in Accra, Ghana.

(A) (B)

Figure 3.0.Image showing: (A) Riped *Musa sp.* and (B) Fruits of *Tetrapluera sp.*

3.2.2.2. Drying of Plant materials

The fresh plant materials were cut into smaller sizes and were thoroughly washed with deionized water. Subsequently, they were air-dried for about two weeks. For effective grinding, the chopped plant materials were further dried using an oven drier at a temperature of 60^{o}C until no further loss in weight.

3.2.2.3. Milling of Plant materials

Plant materials were ball milled using an attrition milling machine in our laboratory. The triturated plant materials were sieved with a 150 micron-sized mesh to obtain much finer powdered materials.

3.2.2.4. Extraction process

30g of each powdered sample was mixed with 2:1 portions of ethanol and water respectively to give a 30ppm extract solution. To obtain highly viscous extracts, the mixture was boiled at 80 ° C for 60 minutes under constant stirring. The solution was kept for cooling at room temperature. The cooled mixture was subsequently filtered using a Whatman No.1 filter paper to remove the solid materials present. The extracts were then stored in a refrigerator until further use.

Table 3.1. Summarized experimental details.

Name of species	Part of plant	Temperature	Time for boiling	Colour of the solution	
				Before	After
Tetrapleura sp	Fruits	80 ^{o}C	60 mins	Light brown	Deep brown
Musa sp	Peels	80 ^{o}C	60 mins	Brown	Deep brown

3.2.3. Phytochemical screening of extracts

Phytochemical analysis of the plant extracts used in the current work was carried out as done in (Bashair H Al Kinani, 2017). Various phytochemicals such as polyphenols, flavonoids, saponins and tannins were tested for in extracts of *Tetrapleura sp.* and *Musa sp.*

3.2.3.1. Test for polyphenols (Ferric chloride test)

Approximately 1 ml of 80% hydro-ethanol extract from each plant was placed in a test tube accompanied by 3 drops of 10% aqueous ferric chloride and 3 drops of sodium ferrocyanide respectively. A sudden appearance of blue colouration indicates the existence of polyphenols.

3.2.3.2. Test for flavonoids (Alkaline reagent test)

Out of 80 % hydro-ethanolic extract of plant material, 2 ml was poured into a test tube, and about 5 ml each of dilute NaOH and HCl were added respectively. A change from yellow to colourless upon additions of NaOH and HCl respectively signifies the availability of flavonoids.

3.2.3.3. Test for tannins (Braymer's test)

40 ml of 80 % hydro-ethanolic extract of each of the plant materials used in the present study was put into a test tube and boiled. This was filtered, and then 0.1% ferric chloride ($FeCl_3$) reagent was added to the filtrate. The appearance of a blue-black colouration affirms the presence of tannins.

3.2.3.4. Test for saponins (Foam test)

About 40 ml of 80 % hydro-ethanolic extract was agitated in a test tube and warmed in a water bath. Formation of a stable froth indicates the presence of saponins.

3.2.3.5. Test for terpenoids (Salkowki's test)

2.5 ml of the hydro-ethanolic extract of each plant was mixed with 1ml of chloroform in a test tube and 2.5 ml of sulfuric acid was added to the mixture. The formation of a layer of reddish-brown colouration indicates the existence of terpenoids.

3.2.3.6. Test for glycosides (Keller kiliani test)

2.5 ml of the hydro-ethanolic extract of *Musa sp.* and *Tetrapleura sp.* were put into separate test tubes. Into each test tube, 1 ml of glacial acetic acid together with a drop of ferric chloride was added. 0.5 ml of sulfuric acid was then added to the mixture in each test tube. The appearance of a brown ring at the base of the tube indicates a positive test for glycosides.

3.2.4. Preparation of iron nanoparticles (FeNPs)

Iron nanoparticles (FeNPs) were synthesized using each of the extracts separately, by adding the extracts dropwise to 0.1 M $FeCl_3.6H_2O$ in a volume ratio of 1:2 respectively at room temperature. The metal iron solution was prepared by dissolving an appropriate amount of its hexahydrated chloride ($FeCl_3.6H_2O$) salt in deionized water. The addition of the extract to the aqueous ferric solution was done slowly with constant stirring of the resulting mixture for 15 minutes using a magnetic stirrer. Nanoparticles formation and growth were initially confirmed through visual inspection of colour changes. The mixture was left to stand for another 15 minutes prior to centrifugation. The synthesis was done at the original pH (2.5) of the mixture and at room temperature. The biosynthesized nanomaterials obtained using extracts of *Tetrapluera sp* and *Musa sp* were identified as FeNPs-TE and FeNPs-MU, respectively. The as-prepared nanomaterials were fully characterized using microscopic and spectroscopic techniques.

Table 3.2. Summary of experimental details on nanoparticle synthesis.

Name of FeNPs	Plant extract	Temperature of synthesis	Time for stirring	Colour of final solution
FeNPs-TE	*Tetrapleura sp.*	25 ^oC	15 mins	Black
FeNPs-MU	*Musa sp.*	25 ^oC	15 mins	Black

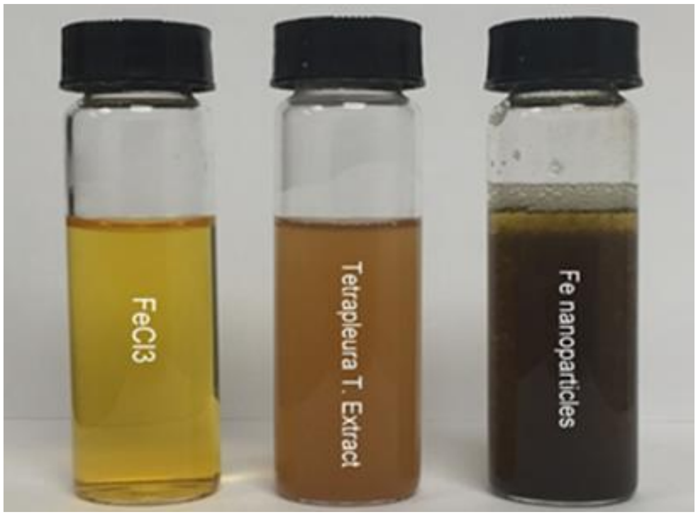

Figure 3.1. (left to right) 0.1 M $FeCl_3$ solution, liquid extract of *Tetrapleura sp.*and freshly prepared FeNPs-TE at room temperature

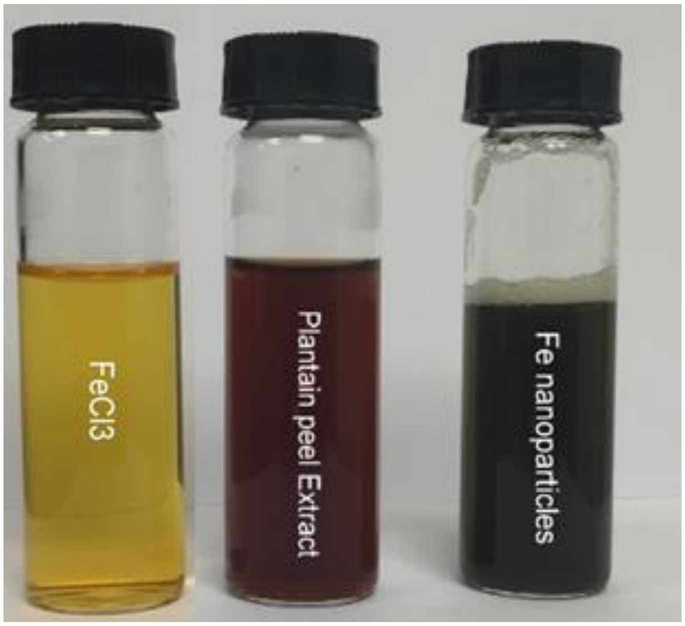

Figure 3.2. (left to right) 0.1 M $FeCl_3$ solution, liquid extract of *Musa sp.* and freshly prepared FeNPs-MU at room temperature.

3.2.5. Characterization of FeNPs

Morphological studies on the prepared nanomaterials were done using a transmission electron microscope (TEM). The TEM images were obtained using a Hitachi H-8000 TEM microscope. UV-Vis analysis was done using UV-1800 spectrophotometer in a spectral range of 200-800 nm. The crystallinity of the as-prepared nanomaterials was examined using powder XRD analysis with a computer-controlled X-ray diffractometer. The FTIR spectra of the prepared nanomaterials and extract were obtained using the Perkin–Elmer spectrophotometer. A measure of stability (zeta potential) of the colloidal solution of nanoparticles was done by dynamic light scattering.

3.3. Results and Discussion

The synthesis of the iron nanomaterials proceeded with simultaneous formation of stable colloidal solutions with distinct colour changes (Figures 3.1 and 3.2). The aqueous extracts of both *Tetrapleura sp.* and *Musa sp.* initially possessed brown colourations. However, on adding the extracts to the aqueous $FeCl_3.6H_2O$ solution yielded a deep black solution. This is an indication of the reduction of Fe^{3+}, due to the excitation of electrons (Sravanthi *et al.*, 2018). Also, the deep black colour of the colloidal solution remained unchanged with time, suggesting the presence of enough nucleation agents responsible for directing nanoparticles formation.

3.3.1. Phytochemical analysis

Results obtained from the phytochemical qualitative analysis performed on the extracts of *Musa sp*. and *Tetrapleura sp*. indicated the presence of saponins, glycosides, tannins and flavonoids in both extracts. However, terpenoids and polyphenols were only present in *Musa sp.* and *Tetrapleura sp*. extracts, respectively (Table 3.3). The combination of these different phytochemicals imposes collective reducing properties which helps the production of the iron nanomaterials by reducing the precursor Fe^{3+} salt. Generally, flavonoids and polyphenols possess antioxidant and chelating (complexing) properties helped by the hydroxyl groups present. Phenolic derivatives are important for free radical scavenging abilities (Devatha *et al.*, 2016). The confirmation of the existence of these phytoconstituents in the extracts used in the present study mediated the production of stable and very reactive iron nanomaterials as, FeNPs-TE and FeNPs-MU.

Table 3.3. Results of phytochemical screening of plant extracts.

Name of test	Phytochemical	*Musa sp.*	*Tetrapleura sp.*
Ferric chloride test	Polyphenols	−	+
Alkaline reagent test	Flavonoids	+	+
Braymer's test	Tannins	+	+
Foam test	Saponins	+	+
Salkowki's test	Terpenoids	+	−
Keller killiani test	Glycosides	+	+

3.3.2. Characterization of iron nanoparticles (FeNPs)

3.3.2.1. Fourier Transform Infrared Spectroscopy (FTIR)

FTIR was employed in this study to ascertain the surface composition of the synthesized iron nanomaterials, particularly the specific functional groups which may contribute to the formation of FeNPs. Thus, the technique in effect provides information on the interaction between the phytochemicals available in the plant extracts and metal ions responsible for the production and capping of the iron nanoparticles. This was confirmed in terms of the individual band intensities observed in the extracts and their corresponding nanoparticles (Figures 3.4 and 3.5). Although the nanoparticles possessed similar absorption peaks like that of the extracts, the differences in intensities suggest the importance of functional groups in the reduction and capping processes. Based on the results obtained (Figures 3.4 and 3.5), it was observed that the synthesized iron nanomaterials had phenolic O-H stretch, C-H and CH_2 vibration of aliphatic hydrocarbons, C=C stretch of ketone, C-O stretch of alcohol as the predominant functional groups. These results are in agreement with that reported by (Devatha *et al.*, 2016). For FeNPs-TE, bands at 3330.21 cm^{-1} representing O-H stretching vibration, 2937.02 cm^{-1} for C-H and CH_2 vibration of aliphatic hydrocarbons, 1621.16 cm^{-1} for C=C stretch of ketone, 1216.11 cm^{-1} for C-O stretch of ester and 1075.13 cm^{-1} for C-O stretch of alcohol were observed. Similarly for FeNPs-MU, bands at 3333.10 cm^{-1} suggesting O-H stretching vibration, 2926.38 cm^{-1} for C-H and CH_2 vibration of aliphatic hydrocarbons, 1615.07 cm^{-1} for C=C stretch of unsaturated ketone and 1071.61 cm^{-1} for C-O stretch of primary alcohol were observed. Clearly, it was noticed that absorption bands for the predominant functional groups were similar on the surfaces of both nanomaterials. This could be as a result of similarities in functional groups possessed by the dominant phytochemicals in the extracts (Figure 3.3). Also, the spectra for both extracts showed similarities in positions of absorption peaks, albeit considerable differences in peak intensities were observed (Figure 3.3). The peak intensities of the active functional groups in *Tetrapleura sp.* were higher than those of *Musa sp.*, suggesting a higher concentration of functional groups. The presence of these mixed functional groups may contribute to the production and stabilization of the iron nanomaterials. Hence, the formation of FeNPs is largely envisaged to be due to the presence of a plethora of polyphenolic compounds which will cause the reduction of Ferric ions (Smuleac *et al.*, 2011).

A general reaction can be written as :

$nFe^{3+} + 3Ar-(OH)_n \rightarrow nFe^0 + 3Ar{=}O + 3nH^+$

where Ar is the phenyl group and n is the number of hydroxyl groups oxidized by Fe^{3+}

Table 3.4. Predominant absorption bands obtained through Fourier Transform Infrared (FTIR) spectrum for the synthesized iron nanomaterials.

Name of FeNPs	Wavelength	Functional group
FeNPs-TE	3330.21 cm^{-1}	O-H group
	2937.02 cm^{-1}	C-H and CH_2 of aliphatic hydrocarbons.
	1621.16 cm^{-1}	C=C stretch of ketone
	1216.16 cm^{-1}	C-O stretch
	1075.13 cm^{-1}	C-O stretch of primary alcohol
FeNPs-MU	3333.10 cm^{-1}	O-H group
	2926.38 cm^{-1}	C-H and CH_2 of aliphatic hydrocarbons
	1615.07 cm^{-1}	C=C stretch of unsaturated ketone
	1071.61 cm^{-1}	C-O stretch of alcohol

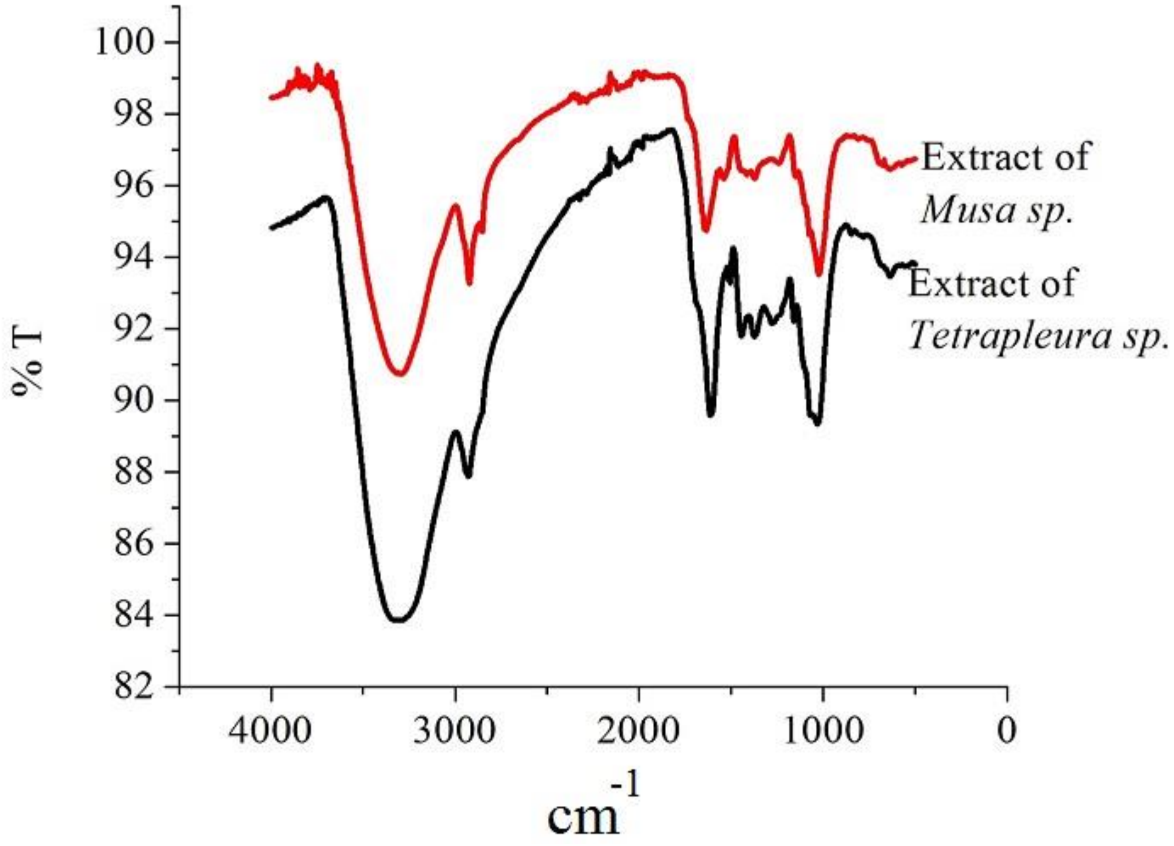

Figure 3.3. FTIR spectra for extracts of *Musa sp. and Tetrapleura sp*.

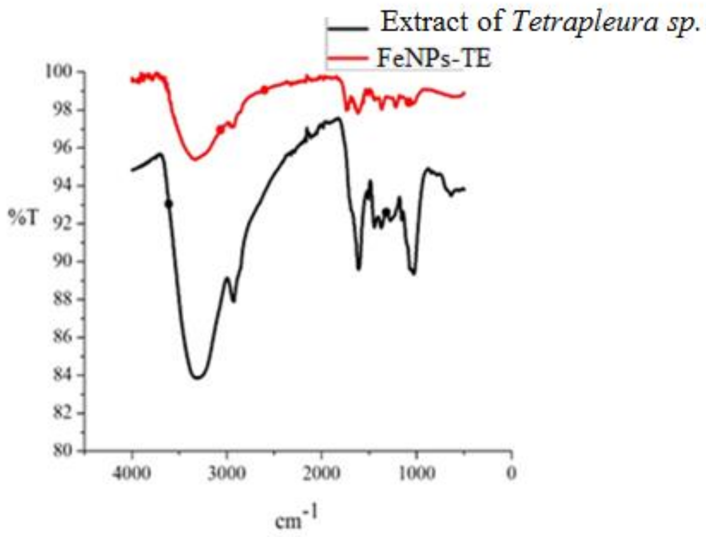

Figure 3.4. FTIR spectra for extract of *Tetrapleura sp.* and FeNPs-TE

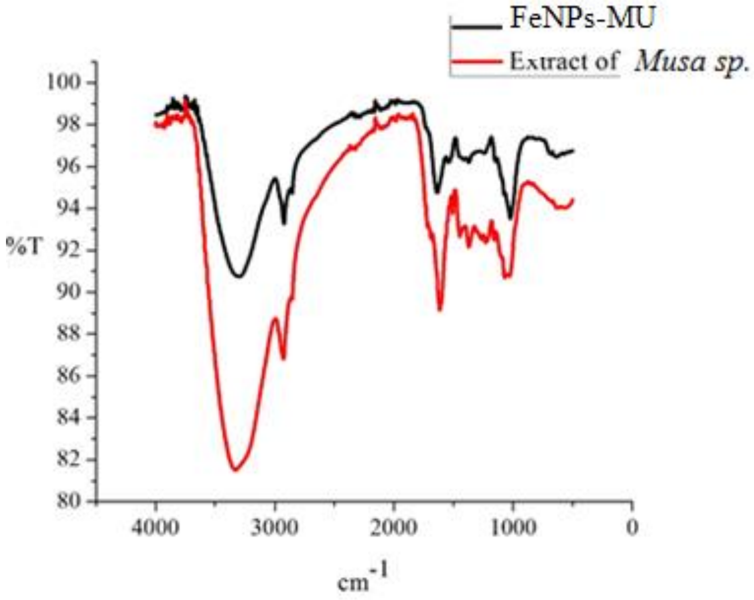

Figure 3.5. FTIR spectra for extract of *Musa sp.*and FeNPs-MU

3.3.2.2. Ultraviolet-visible Spectroscopy (UV-Vis)

In recent times, UV-Vis absorption spectroscopy has appeared as the most widely used tool to characterize nanomaterials' optical characteristics. The intensity and position of the surface plasmon resonance (SPR) band of the nanomaterial are linked to the size, shape and agglomeration state of the nanomaterials (Wang & Ni, 2014). The UV-Vis spectra obtained for the iron nanomaterials (FeNPs-MU) and that of the extract of *Musa sp.* differed with positions of maximum peaks (Figure 3.6). Direct comparison of the two spectra shows a peak or kink positioned at 300 nm in A**,** which is the characteristic SPR band for metallic iron nanoparticle (Katata-Seru *et al.*, 2017). The spectrum of the extract of *Musa sp.* showed no such peak suggesting that, the observed spectrum, B may be as a result of free phytochemicals present in the extract. Similarly, the spectrum for FeNPs-TE showed a maximum absorption band at a wavelength of 300 nm, typical of nanoscale iron (Figure 3.7). The spectrum obtained for the plant extracts was the same (that is B in Figures 3.6 and 3.7). This may suggest that both extracts may contain similar free phytochemicals which were responsible for nanoparticle formations.

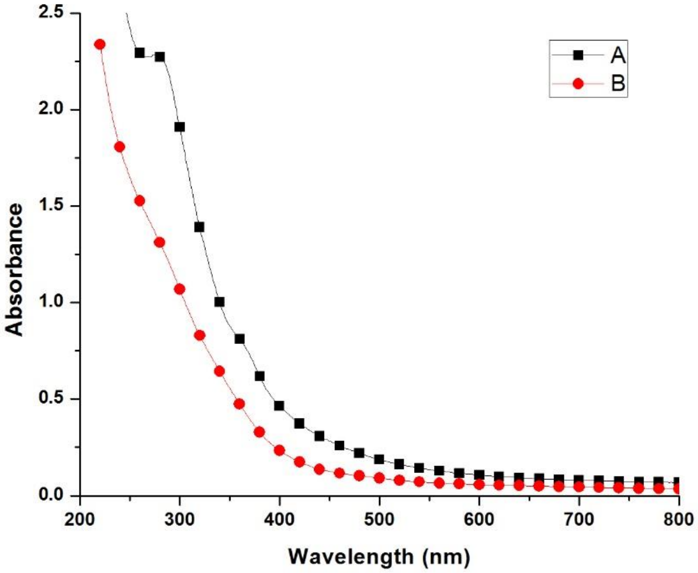

Figure 3.6. UV-Vis spectra of (A) FeNPs-MU and (B) extract of *Musa sp.* at room temperature.

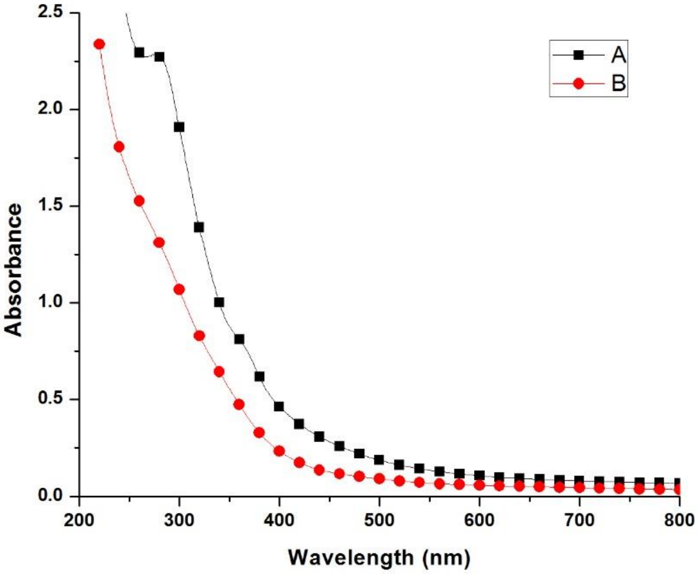

Figure 3.7. UV-Vis spectra of (A) FeNPs-TE and (B) extract of *Tetrapleura sp.* at room temperature.

3.3.2.3. Transmission electron microscope (TEM)

The size and morphology of biosynthesized FeNPs-MU and FeNPs-TE at room temperature were determined by TEM, as shown in Figures 3.8. and 3.9. Obtained TEM micrographs of freshly prepared FeNPs-MU (Figure 3.8.) and FeNPs-TE (Figure 3.9) revealed that particles had uniform sizes and are of a definite shape. FeNPs-MU were cylindrically shaped particles with dimensions of about 80 nm (Figure 3.8.). As expected, the uniformity and the monodispersed nature of the FeNPs-MU particles may present them as good candidates for environmental remediation. Primarily**,** Figure 3.9 shows the TEM images of FeNPs-TE. The images suggest that, the microstructure of the synthesized nanomaterials could best be described as particles of nano dimensions which are continuously linked to each other. The continuous way of particle arrangement of FeNPs-TE implies, their catalytic ability would proceed in a non-discrete manner, which is an indication that particles may hold good promise for environmental remediation. This assumption was explored in the degradation of Vat orange dye. Results from this study are discussed in the succeeding chapter.

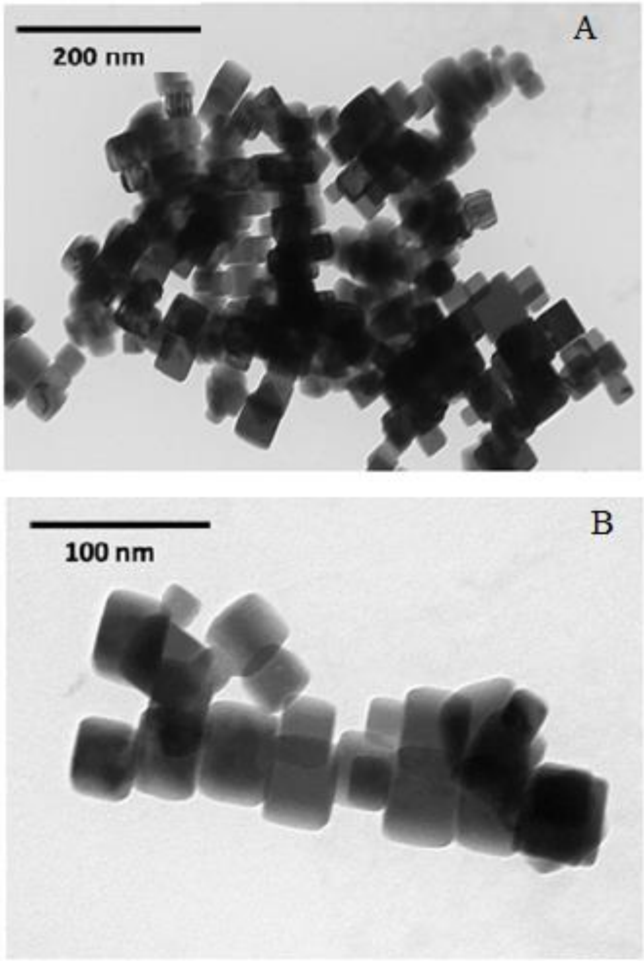

Figure 3.8. TEM images of FeNPs-MU at (A) low magnification (B) high mgnification at room temperature and at original pH.

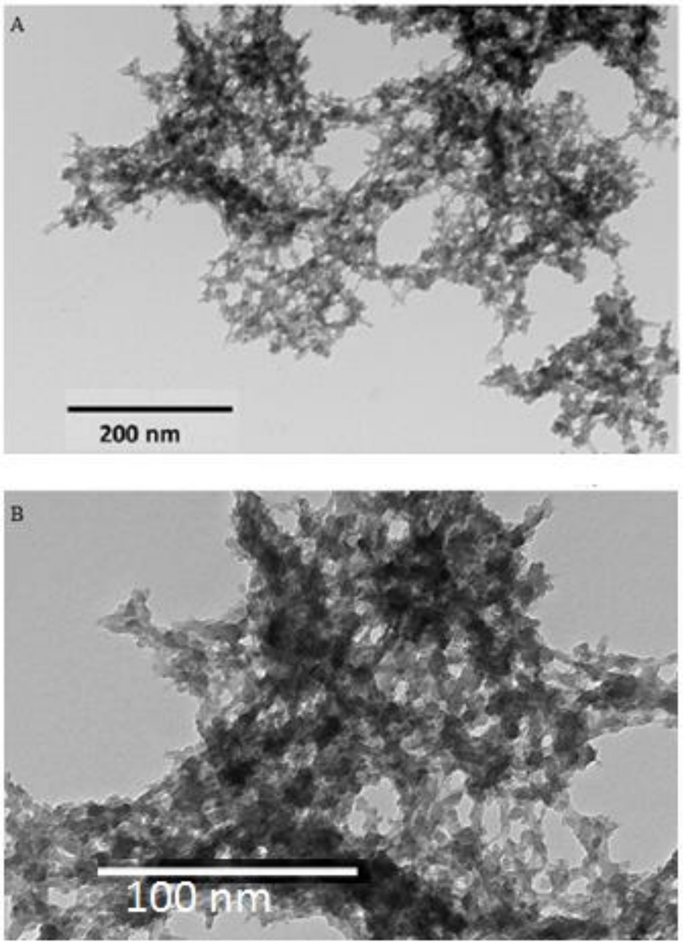

Figure 3.9. TEM images of FeNPs-TE at (A) low magnification (B) high magnification at room temperature and original pH.

3.3.2.4. X-ray diffraction (XRD) analysis

Powder XRD analysis was employed to investigate the surface crystallinity of the biosynthesized iron nanomaterials and also ascertain the oxidation state of the iron metal core in the prepared nanomaterials. Nanoparticles obtained from both extracts; FeNPs-TE and FeNPs-MU were subjected to XRD analyses over a two theta (2θ) range of about 0 to 80 ^{o} and 0 to 60 ^{o} respectively. The XRD pattern for FeNPs-MU showed no peaks (Figure 3.10.), most importantly, the characteristic peak of zero-valent iron at $2\theta = 44.8^o$, suggesting that the green synthesized FeNPs-MU is amorphous in nature. This is in agreement with other studies (Machado *et al.*, 2015). The absence of the much sought-after peak at $2\theta = 44.8^o$ could be as a result of a thick layer of organic compound from the Musa *sp*. extract which may have blanketed the iron core of the nanomaterial, thus making the Fe^0 peak undetectable (Machado *et al.*, 2015). Also, this may be an indication of well capped FeNPs-MU by the organic compounds present in the extract. Figure 3.11 is the XRD pattern for FeNPs-TE. A peak at $2\theta = 44.8^o$ among other peaks were observed (Figure 3.11). The peak at 44.8 ^{o} is attributable to the characteristic peak of zero-state valent iron, which appeared to be the dominant oxidation state of iron, in the biosynthesized FeNPs. The other peaks may be as a result of impurities which accompanied the nanomaterials during synthesis.

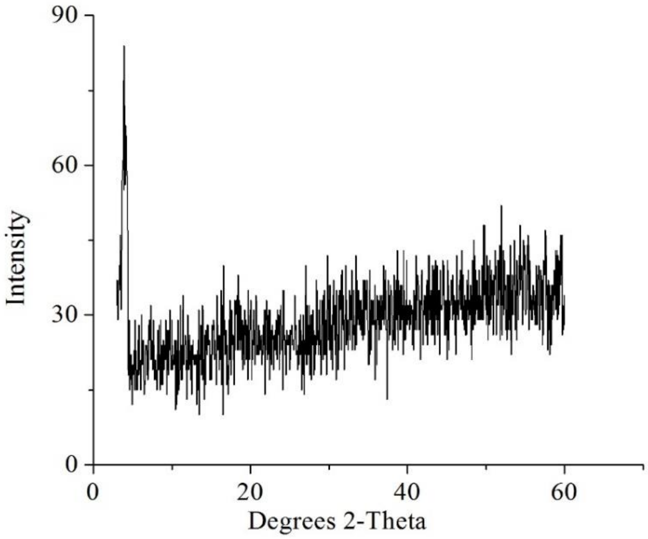

Figure 3.10. X-ray diffraction (XRD) pattern for FeNPs-MU

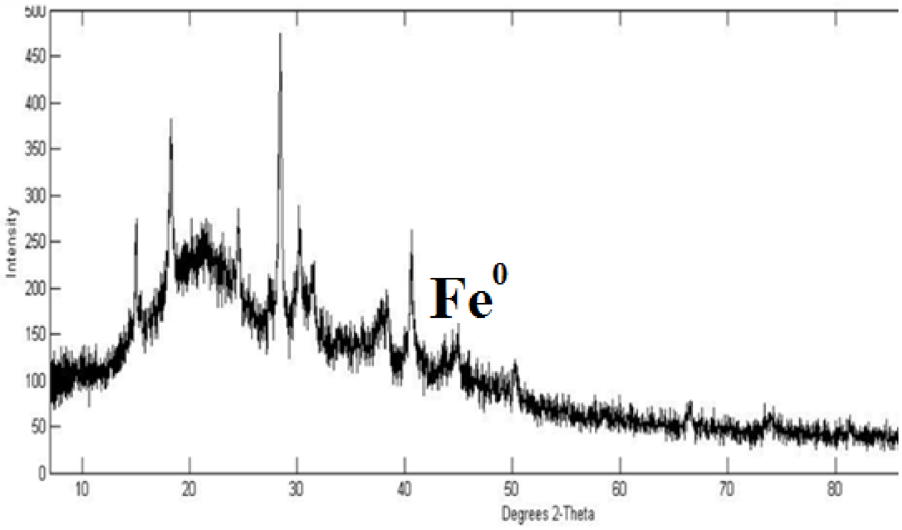

Figure 3.11. X-ray diffraction (XRD) pattern for FeNPs-TE

3.3.2.5. Dynamic Light Scattering (DLS) Analysis

Dynamic Light Scattering (DLS) is a technique employed to investigate the particle size and zeta potential of small particles in a colloidal solution. Zeta potential remains a concept that is key to revealing the stability of small particles in a colloidal solution or suspension (Uskokovic *et al.*, 2011). In the present study, dynamic light scattering was used as the sole technique to measure the stability of the biosynthesized iron nanomaterials (FeNPs-TE and FeNPs-MU). Literature indicates that, the higher the zeta potential of a particle in a colloidal solution, the more stable it is, as illustrated in Kumar *et al.*, (2017). In other words, the stability of small particles in a colloidal solution is directly proportional to the value of its zeta potential. Results suggested that, the two biosynthesized iron nanomaterials displayed varying stability. Per the zeta potential values, FeNPs-MU particles were highly stable compared to FeNPs-TE particles (Table 3.4). This may imply that, the hydroxyl groups in the phytochemicals present in *Musa sp.* extract strongly capped the nanoparticles. The decrease in stability of FeNPs-TE may be as a result of weak interactions that existed between the hydroxyl groups from the *Tetrapleura sp*. extract and the metal core of the nanoparticle. The XRD pattern for FeNPs-MU suggested that the surface of the particles had a thick layer of organic compounds, and this corroborates the obtained zeta potential value. The table below gives the obtained zeta potential values of the 'as synthesized' FeNPs with their stability description based on Kumar *et al.*, (2017).

Table 3.4. Zeta potential values for FeNPs-TE and FeNPs-MU

Name of FeNPs	Zeta potential [mV]	Stability of behaviour of the colloid
FeNPs-TE	16.6	Less stability
FeNPs-MU	32.03	Good stability

3.4. Conclusions to Chapter Three

The synthesis of FeNPs was accomplished by using the peel and fruit extracts of *Musa sp*. and *Tetrapleura sp*., respectively. The phytochemical constituents of these extracts served as both reducing and capping agents. The biosynthesized iron nanomaterials (FeNPs-TE and FeNPs-MU) were prepared at ambient conditions. FTIR results confirmed the presence of predominant hydroxyl groups in extracts responsible for capping of iron nanomaterials. UV-Vis results also confirmed the synthesis of FeNPs by showing a band at 300 nm, typical of nanoscale iron. The prepared nanoparticles possessed varying levels of stability with FeNPs-MU particles showing better stability.

This, therefore, provides an alternative route to the synthesis and stabilization of iron nanomaterials.

CHAPTER FOUR

4.0. Degradation of Vat orange dye using bio-synthesized iron nanoparticles (FeNPs)

4.1 Introduction to Chapter Four

Nowadays, it is more than palpable that the pristine nature of our environment is in a compromised state due to industrialization and other anthropogenic activities giving rise to several environmental and human health challenges. The problem is compounded by the ever-increasing release of various pollutants, some of which are persistent in the environment.

Effluents from industries such as textile, paint, printing, food, ceramics, paper, and pharmaceutical are a source of considerable contamination including organic waste such as synthetic dyes (Rebitanim *et al.*, 2013; Wanyonyi *et al.*, 2014). These dye residues, when present in wastewater, impart their characteristic colour to receiving waters leading to the production of coloured contaminants (Sravanthi *et al.*, 2018). Additionally, degradation of azo dyes in the absence of oxygen induces the formation of carcinogenic and highly toxic amines posing significant risks to aquatic life (Sravanthi *et al.*, 2018). The need for effective treatment processes for industrial effluents before their disposal into surrounding water bodies is vital. A good number of biological, chemical and physical processes have been established to remediate environmental pollution, including water pollution. Some of these processes include filtration, microbial degradation, membrane separation and coagulation (Chu *et al.*, 2012; Tian *et al.*, 2008; Yu *et al.*, 2016). However, all these methods are often expensive and less effective. Quite often, the degradation of synthetic dyes has been achieved through photo-catalytic processes. On the contrary, these photo-catalytic processes sometimes lead to the formation of toxic intermediates suggesting the need for alternative safer mechanisms (Bishnoi *et al.*, 2018).

Nanotechnology has emerged as a promising strategy for wastewater remediation in a more potent and efficient approach (Shen *et al.*, 2009, T. Wang *et al.*, 2014). In recent years, nano-sized materials have evinced their application in the provision of clean and cost-effective wastewater treatment technologies. Exclusive features of nanomaterials including high surface area and mechanical properties, good chemical reactivity, low cost, and efficient regeneration for reuse have promoted nanomaterials as a promising tool for environmental remediation (Pavan Kumar Gautam, 2019).

Currently, iron nanomaterials remain the most widely used nanomaterials for the treatment of contaminated soil and water. This is because, iron nanoparticles tend to follow the maximal green chemistry principles as an inexpensive, non-toxic and environmentally compatible material (Li *et al.*, 2006). At the same time, iron is very reactive and readily available. The core shell of the iron nanoparticles confers unique redox properties on them, presenting them as good candidates for the reduction of contaminants (Yan *et al.*, 2010). According to Sravanthi *et al.*, (2018), iron reacts with water to form a film of oxide called goethite (FeOOH) which has an immense affinity for contaminants. This establishes a nimble reaction between FeNPs and the contaminants expediting the removal process. Iron nanoparticles (FeNPs), among other nanostructures have acted as effective bio-catalysts for the degradation of methylene blue dye (Ohemeng *et al.*, 2020) as well as other environmental contaminants including radioactive elements like uranium and plutonium (Crane *et al.*, 2015).

In lieu of this, the current study focuses on the catalytic application of synthesized FeNPs prepared from extracts of Plantain peel (*Musa sp.*) and “Prekese” (*Tetrapleura sp.*) on the degradation of locally used Vat dyes.

4.2. Materials and Methods

4.2.1. Reagents and equipment

The as-prepared iron nanomaterials (FeNPs-MU & FeNPs-TE) used in this current study were synthesized by adhering to the processes outlined in **chapter 3**. The dye employed in the study was of analytical reagent grade and purchased from Sigma Aldrich.

4.2.2. Batch experiments of dye decolourization.

Experiments for the decolourization of the dye were set up at room temperature and at the pH of the individual FeNPs-dye mixtures as adopted by Sravanthi *et al.*, (2018). Here, 24 mg of iron nanomaterials each from FeNPs-MU & FeNPs-TE was mixed with 50 ml of 30 ppm dye solution in separate containers. The mixtures were stirred using a magnetic stirrer. At time intervals of 5, 10, 15, 20, 25, 30, 40, 50, 60, 90, 120, 180, and 240, aliquots were taken and analysed using a spectrophotometer. This was done to ascertain the effect of contact time on the degradation process. Other synthetic conditions such as pH, temperature, initial adsorbate concentration and adsorbent dosage were varied and optimized to investigate their influence on the adsorption process. The concentration of each dye remaining in solution was determined spectrophotometrically by measuring absorbance at 665 nm (typical wavelength for dye absorption). The changes in the dye solution concentration were computed from the difference between the initial concentration and the final dye solution concentration in equilibrium. The adsorption capacity of dye on adsorbent was calculated using the equation below:

$$q_e = \frac{(C_o - C_e)\,V}{W}$$

where C_o and C_e are the dye concentrations (mg/L) initially and at a given time, t respectively; V, volume of dye solutions (L); W, weight of adsorbent, (g). Also, the sorption efficiency or removal efficiency of the adsorbent was calculated from the equation below:

$$\textbf{\textit{Percentage of removal}} = \frac{(C_o - C_e).\ 100}{C_o}$$

where C_o and C_e are initial and equilibrium concentrations of dye solution respectively

4.3. Results and Discussion

4.3.1. Characterization of Sorbent

As earlier documented in the preceding chapter (Chapter 3), **Figures** 3.8 – 3.9 showed the TEM images of freshly synthesized iron nanomaterials. It was found that, the FeNPs possessed nano dimensions with FeNPs-TE showing inter-particle linkages and diameter dimensions ranging from 80 – 100 nm.

UV-Vis analyses of the biosynthesized iron nanomaterials showed a maximum absorption peak at 300 nm, which could be attributed to the surface plasmon resonance (SPR) band of nanoscale iron. FT-IR results showed the presence of some organic functional groups that may be responsible for the formation and capping of the nanomaterials.

4.3.2 Effect of synthetic conditions on the sorption capacity of vat orange dye

4.3.2.1. Effect of Contact time

From Figure 4.0, the sorption of vat orange dye increases with increasing contact time. The process, however, attains saturation after 240 minutes of exposure to nanomaterials, beyond which no further reactions were visible. At this point, the adsorption sites present on the FeNPs (adsorbent) surfaces are almost completely covered; hence the removal rate of the dye almost remain unchanged. Fundamentally, this suggests that the adsorption process is rapid but decreases until equilibrium is reached. Also, the percentage removal of the dye increased with increase in contact time, and this is in strong agreement with (Wanyonyi *et al.*, 2014). After 240 min, a percentage dye removal of 82.3% and 64.3% were achieved with FeNPs-TE FeNPs-MU respectively. This appreciably high removal rate observed could be explained by the large surface area that may be available for the dye adsorption. The difference in percentage removal of dye molecules by FeNPs-TE and FeNPs-MU can be accounted for by the different sizes and uniformity shown by the individual as-prepared nanomaterials.

In general, a considerable decrease in the rate of removal of dye molecules is expected at longer contact time of dye treatment with nanoparticles. This is as a result of the adsorbent gradually becoming inundated with the adsorbate over time, leaving behind few vacant surface sites which may remain unoccupied because of a number of repulsive forces that may exist between the dye molecules and nanoparticles (Wanyonyi *et al.*, 2014).

A comparison of the behaviour of adsorbate when treated with each of the biosynthesized iron nanomaterials (FeNPs-TE and FeNPs-MU) suggests that FeNPs-TE performed better with higher adsorption capacity of the dye onto its surfaces. This resulted in a better percentage of dye removal (82.3 %) compared to FeNPs-MU. This higher rate of dye removal may be due to the non-discrete and continuous nature of FeNPs-TE produced as observed from the transmission electron microscope (TEM) images (Figures 3.8-3.11). This continuous nanoparticles greatly enhances adsorption leading to higher removal efficiency.

In addition, the major breakthrough point of FeNPs-TE was observed after 176 minutes, whereas that for FeNPs-MU was after 80 minutes. The breakthrough point is the point where an adsorbent reaches its separation point and hence, cannot adsorb anymore adsorbate. This may suggest that desorption of dye molecules proceeds faster on surfaces of FeNPs-MU than FeNPs-TE, making the latter a better adsorbent.

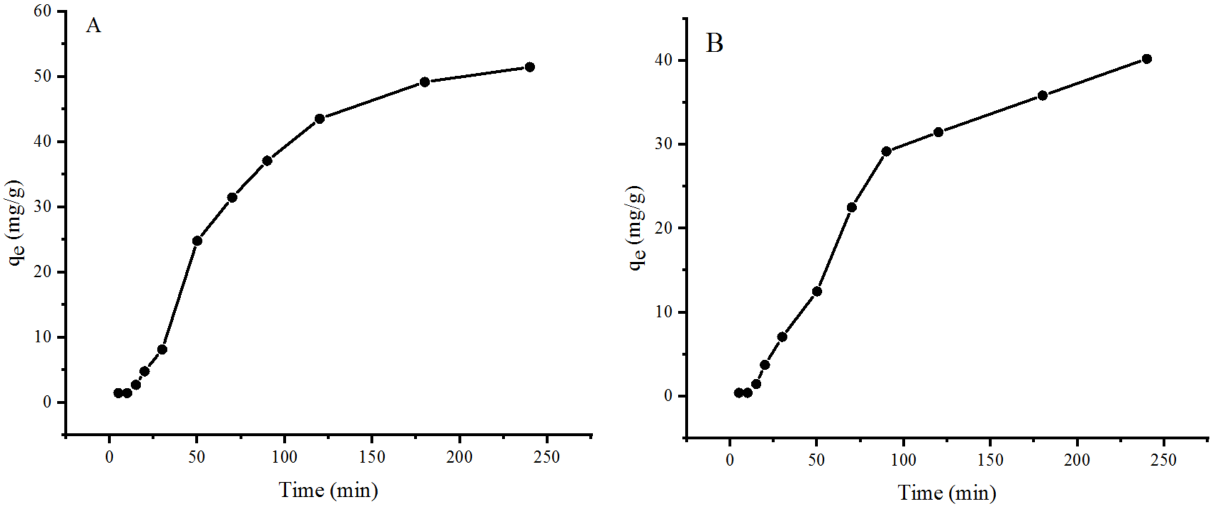

Figure 4.0. Effect of contact time on the adsorption of Vat orange dye on: (A) FeNPs-TE and (B) FeNPs-MU

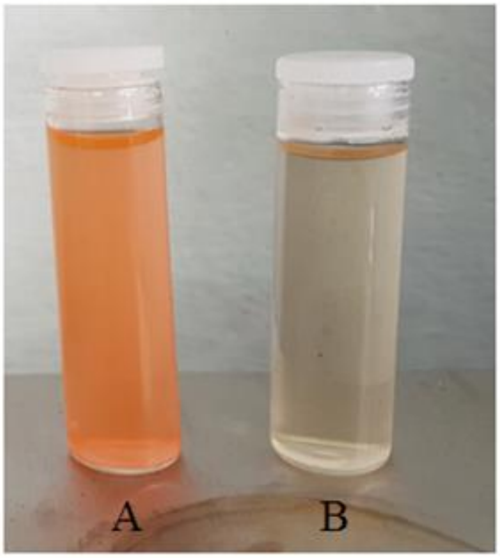

Figure 4.1. Colour changes accompanying degradation of Vat orange dye: (A) dye solution after stirring without nanomaterials for 240 mins, (B) dye solution after stirring with 24 mg of nanomaterials for 240 mins.

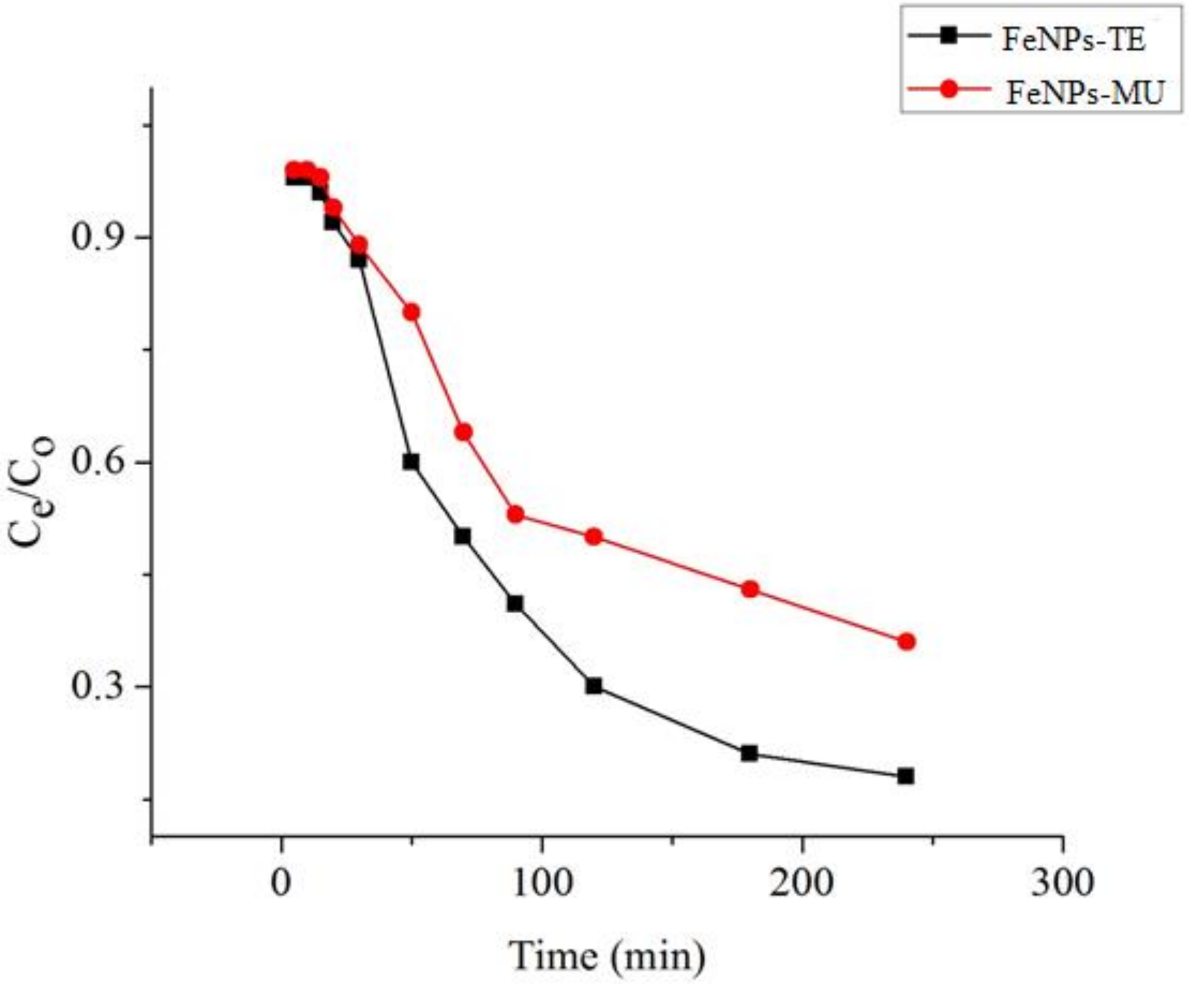

Figure 4.2. Graph showing the breakthrough points of the adsorbents

4.3.2.2. Effect of pH

The impact of pH on the sorption of the dye molecules by the nanomaterials was examined by subjecting 24 mg of adsorbent (FeNPs-TE and FeNPs-MU), to 50 ml of 30 mg/L initial concentration of dye. The initial pH values of the reaction mixtures were adjusted with 0.1 M HCl and 0.1 M NaOH to obtain varying pH values of approximately 5, 7 and 9 (Figure 4.3). A general trend observed in the case of the two different iron nanomaterials utilized suggests that, the adsorption of Vat orange dye is better at lower pH. This could be attributed to the zero point charge of FeNPs (pH_{zpc}). Bishnoi et al. (2018), have shown that the pH of a solution at which the net charge on the FeNPs surface approaches neutral, thus pH_{zpc} is around 8.1 (Bishnoi *et al.*, 2018). This presupposes that, at a low pH ($< pH_{zpc}$), the FeNPs surface possess a positive charge whereas the dye molecules are negatively charged; hence the adsorption of the dye molecules onto the sorbent surfaces is greatly enhanced. Contrarily, at high pH ($> pH_{zpc}$) the adsorption rate is impeded due to the formation of oxides and hydroxides of Fe (II) and Fe (III) which may remain on the sorbent surfaces, inhibiting further reaction. Therefore, acidic conditions may favour the adsorption process. Similarly, (Chen *et al.*, 2011) reported that, the rate of removal of methyl orange dye in an aqueous medium increases with a decrease in pH owing to ionization of FeNPs surfaces whereas the dye remains deprotonated. In the present study, the findings suggest that the synthesized iron nanomaterials equally showed better adsorption of the dye molecules at reduced pH (Figure 4.3).

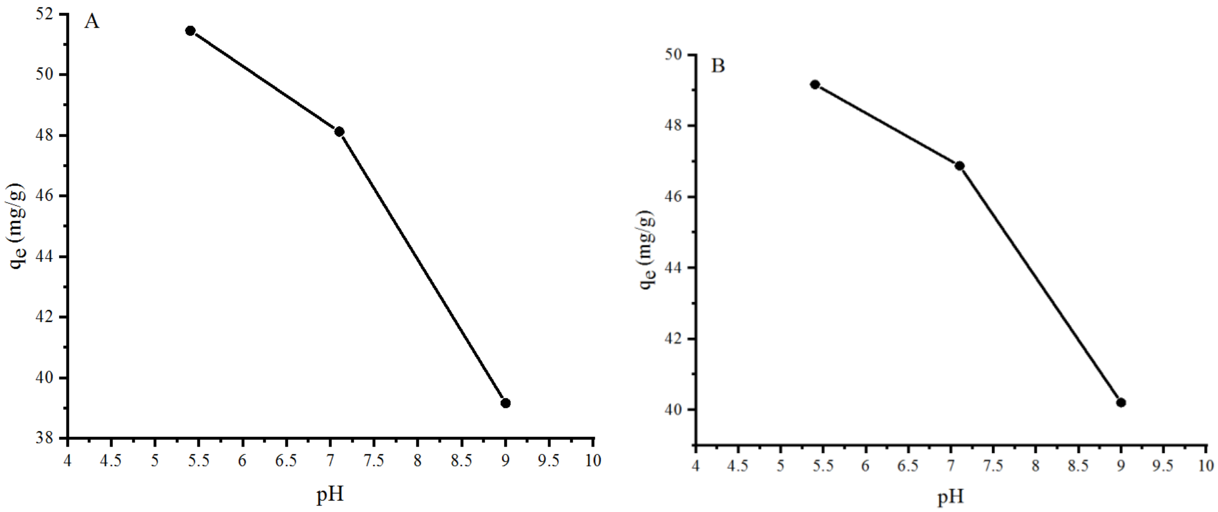

Figure 4.3. Effect of pH on the adsorption of Vat orange dye: (A) FeNPs-TE and (B) FeNPs-MU

4.3.2.3. Effect of temperature

The role of temperature in the adsorption process leading to the removal of dye molecules was investigated by setting up a series of experiments at varying temperatures: 298 K and 318 K (Simin Arabi, 2012). It was observed that, the adsorption capacity of the dye molecules onto the surfaces of the FeNPs sorbents increased with an increase in temperature (Figure 4.4), suggesting an endothermic process. Just as reaction rates are enhanced with temperature increase, the present observation could be as a result of increase in adsorptive interactions between the active sites of the adsorbent and the adsorbate molecules.

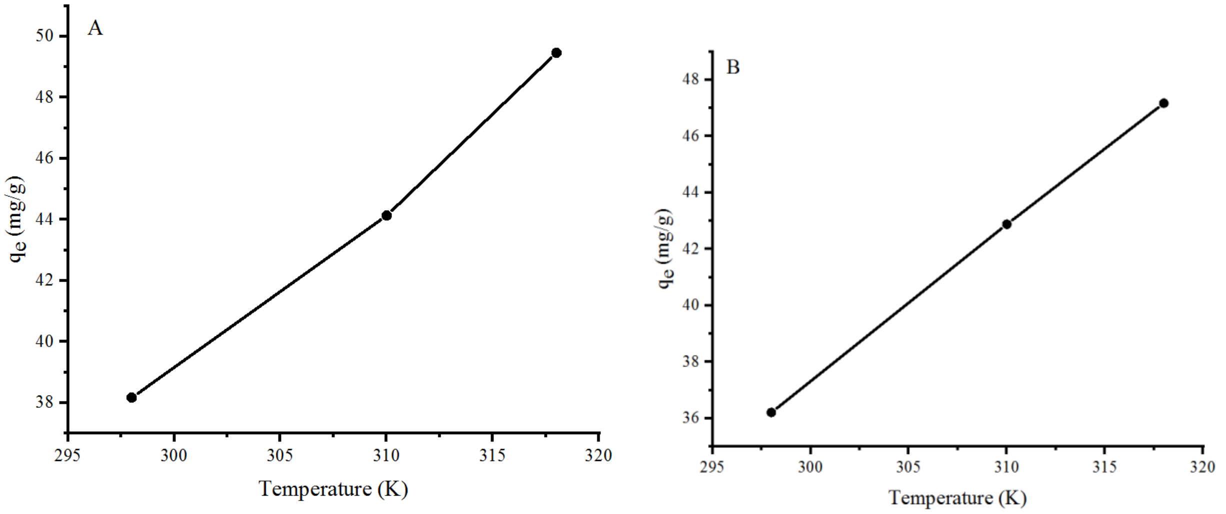

Figure 4.4. Effect of temperature on the adsorption of Vat orange dye: (A) FeNPs-TE (B) FeNPs-MU.

4.3.2.4. Effect of initial adsorbate concentration

The influence of initial dye concentration was investigated at room temperature with varying concentrations ranging from 20 mg/L to 100 mg/L. In all experimental runs, the adsorbent (FeNPs-TE and FeNPs-MU) dose was fixed at 24 mg. The results obtained suggest that the process of dye uptake by FeNPs is dependent on the initial concentration of the Vat orange dye. It was realised that, as the initial concentration of the dye increased, the rate of dye uptake by FeNPs declined (Figure 4.5). This may be attributed to the increase in the number of saturated active sites of FeNPs as a result of the high concentration of dye. Similar trends have been reported for the degradation of methyl orange dye by FeNPs (Chen *et al.*, 2011).

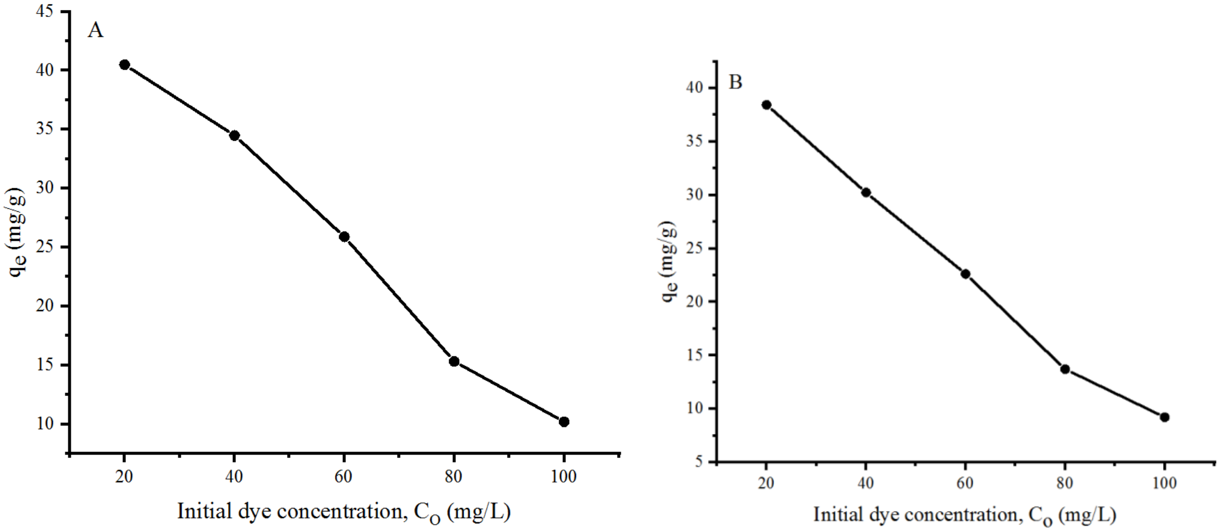

Figure 4.5. Effect of initial concentration of adsorbate on the adsorption of Vat orange dye: (A) FeNPs-TE (B) FeNPs-MU.

4.3.2.5. Effect of adsorbent dosage

The impact of adsorbent dosage on the adsorption of Vat orange dye was carried out at room temperature by varying the amount of adsorbent (both FeNPs-TE and FeNPs-MU) from 5 mg to 25 mg with the initial concentration of the Vat orange dye fixed at 30 mg/L. Generally, the adsorption of the dye onto the adsorbent surface active sites increased rapidly as the amount of FeNPs increased (Figure 4.6). However, this increment was observed up to a point. This observation could be accounted for by the increase in adsorbent surface area with a corresponding increase in the number of available active sites. Although similar trends were observed for the two iron nanomaterials employed, the effect was much pronounced with FeNPs-TE.

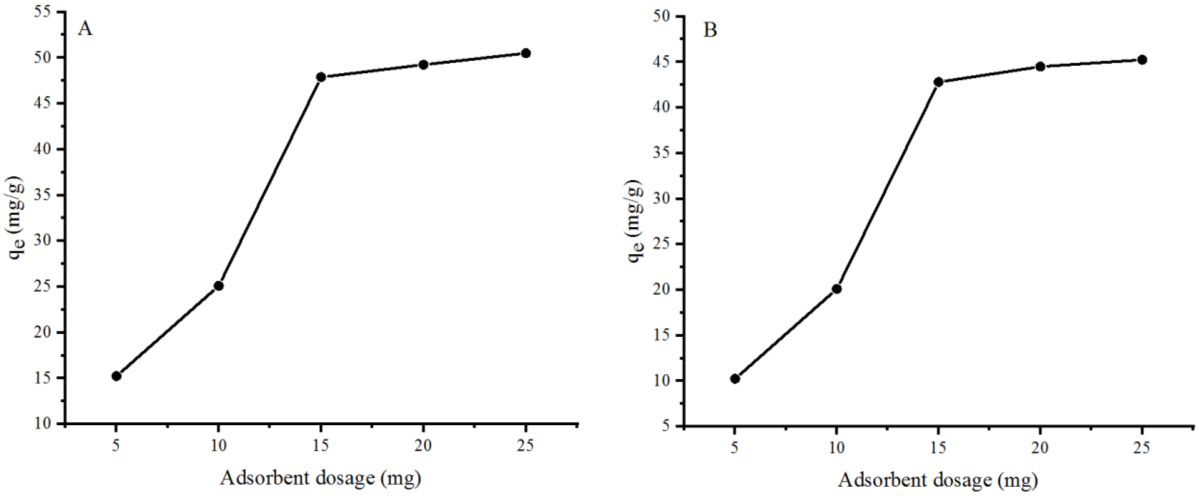

Figure 4.6. Effect of adsorbent dosage on the adsorption of Vat orange dye on: (A) FeNPs-TE (B) FeNPs-MU.

4.3.3. Adsorption isotherms

Equilibrium adsorption isotherms were employed in the current study to help explain the mechanism of the adsorption systems. Langmuir and Freundlich adsorption models were applied and used to interpret the experimental data.

4.3.3.1. Langmuir isotherm

This equilibrium adsorption isotherm model is governed by the assumption that, adsorptions occur at particular homogeneous sites on the adsorbent (Dey *et al*, 2015). Thus, the sorbent surface is made up of identical sites, which possess identical adsorption energies and are equally available for adsorption until a monolayer is formed. The linearized form of Langmuir expression, which establishes the relationship between the molecules covered on a solid surface to the equilibrium concentration of the liquid phase above the adsorbent surface is given by the equation below:

$$\frac{C_e}{q_e} = \frac{1}{K_L\, q_m} + \frac{C_e}{q_m}$$

where q_e (mg g^{-1}) is the amount of dye molecules adsorbed at equilibrium, C_e (mg L^{-1}) is the concentration of dye solution at equilibrium, q_m (mg g^{-1}) is the maximum monolayer coverage capacity and K_L (mg L^{-1}) represents the Langmuir isotherm constant linked to the affinity of the binding sites.

A plot of C_e/q_e against C_e helps to calculate the Langmuir constants (q_m and K_L) as the slope of the graph is $1/q_m$ and the intercept is $1/K_L q_m$. A much pronounced meaning to the Langmuir isotherm equation was realised in terms of calculating for a dimensionless constant, R_L also known as separation factor which is given by:

$$R_L = \frac{1}{1+KC_o}$$

where K is the constant and C_o is the initial dye concentration.

The calculated R_L values give an idea of the shape of the isotherm and further tell whether the isotherm is either favourable ($0 < R_L < 1$), linear ($R_L = 1$) nor unfavourable ($R_L > 1$).

(Figure 4.5) shows the Langmuir adsorption isotherm for Vat orange dye on 24 mg FeNPs-TE and FeNPs-MU respectively. The extremely low correlation coefficients ($R^2 = 0.3407$-0.5674) suggest that the equilibrium adsorptions are not suited well to the Langmuir design, thus the process of adsorption does not support monolayer coverage of dye molecules on the outer surfaces of the two biosynthesized nanomaterials employed. The Langmuir adsorption constants are saummarized in Table 4.1.

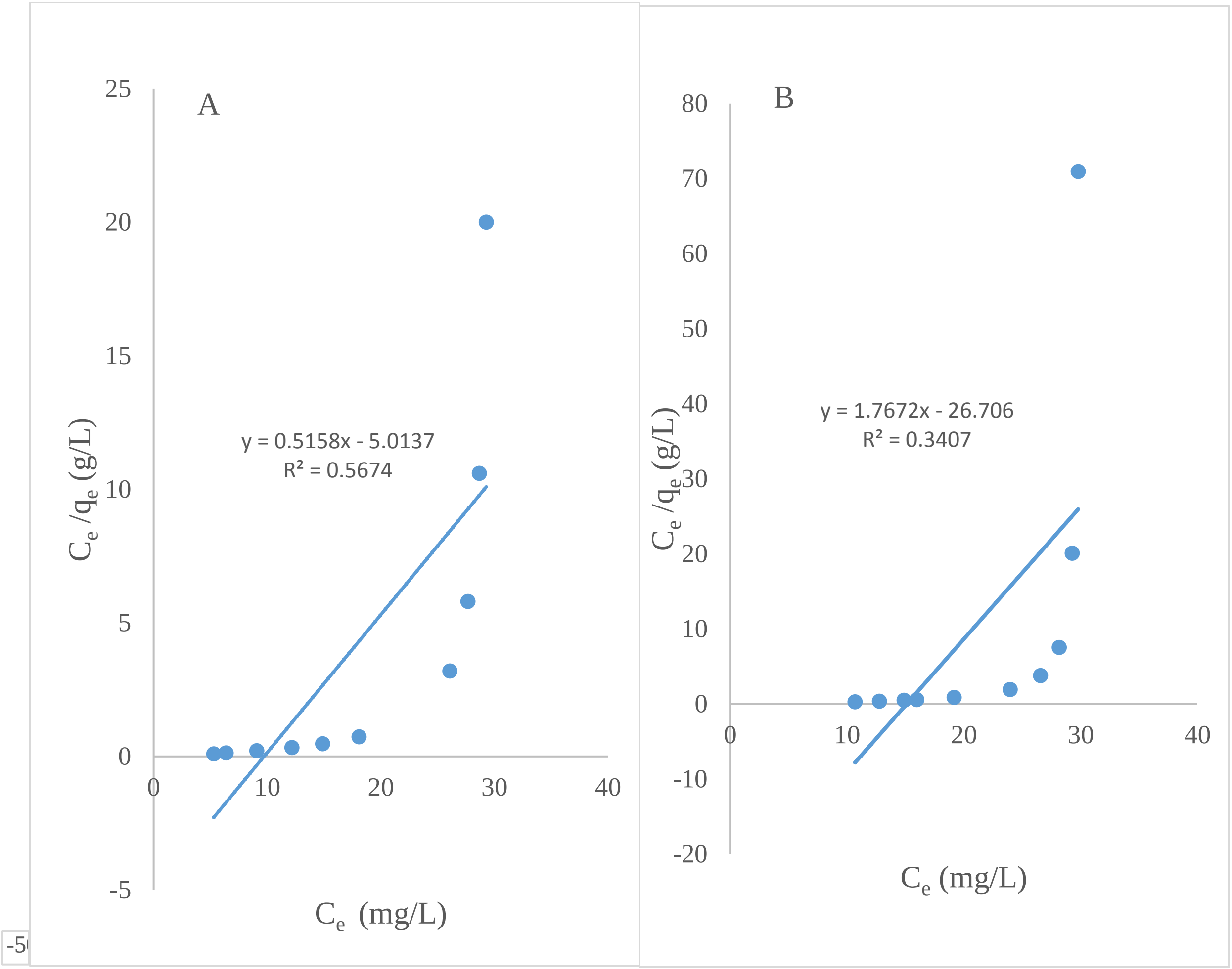

Figure 4.7. Langmuir adsorption isotherm for Vat orange dye on: (A) 24 mg FeNPs-TE (B) 24 mg FeNPs-MU

4.3.3.2. Freundlich isotherm

The linearized form of the Freundlich isotherm equation which is applicable to adsorption on heterogeneous surfaces and multilayer adsorptions is given by:

$$\ln q_e = \ln K_F + \frac{1}{n} \ln C_e$$

where q_e (mg g^{-1}) is the adsorption capacity of dye at equilibrium, C_e (mg L^{-1}) is the equilibrium solute concentration. Invariably, the Freundlich isotherm constants can be extracted from the plot of $ln\ q_e$ versus $ln\ C_e$ where $\frac{1}{n}$ is the slope and lnK_F is the intercept. Essentially, the values for $\frac{1}{n}$ estimate the surface heterogeneity, which gets prevalent as values approach zero. The experimental data fitted a lot better in the Freundlich model based on the higher correlation coefficients (R^2 = 0.7259-0.7640). This presupposes that, the Freundlich isotherm may be applicable for the description of the adsorption of Vat orange dye onto FeNPs surfaces and also an indication of the inherent surface heterogeneity of the biosynthesized iron nanomaterials accountable for multilayer adsorption by the presence of heterogeneous adsorption sites with high energies. While the Freundlich isotherm is a better fit to the data obtained, it may not fully explain the adsorption mechanism given the low correlation coefficients. The use of other isotherms that incorporate more complex and heterogeneous reaction mechanisms may help to fully explain the nature of the interactions occuring.

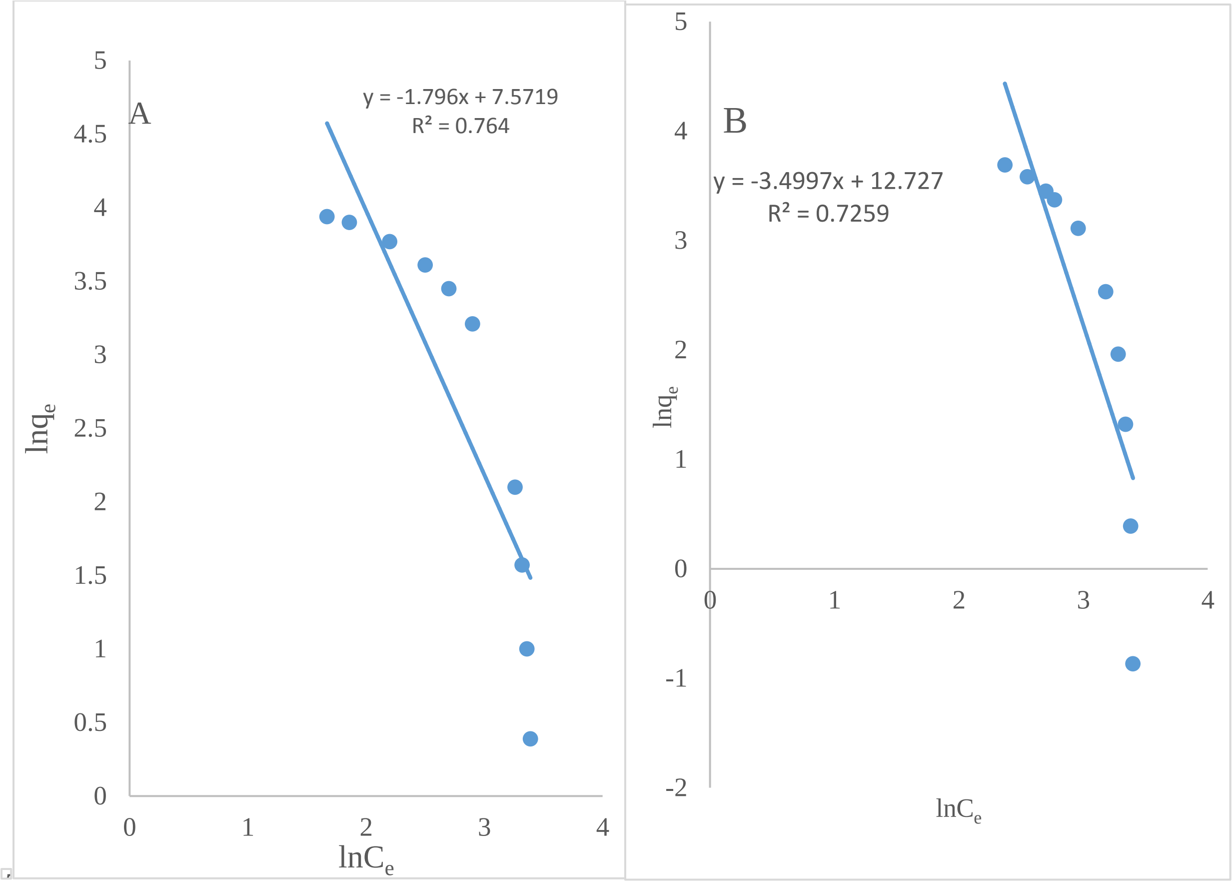

Figure 4.8. Freundlich adsorption isotherm for Vat orange dye on: (A) 24 mg FeNPs-TE (B) FeNPs-MU

Table 4.1. Langmuir and Freundlich isotherm constants for adsorption of Vat orange dye on 24 mg FeNPs-TE and FeNPs-MU.

	Langmuir adsorption isotherm				Freundlich adsorption isotherm		
	K_L	q_m	R^2	R_L	K_F	R^2	n
FeNPs-TE	0.103	1.936	0.566	0.478	3.222	0.759	2.369
FeNPs-MU	0.066	0.566	0.341	1.020	1.236	0.725	0.285

4.4. Conclusion to Chapter Four

The present study has shown that FeNPs can be successfully employed as an adsorbent to quantitatively remove Vat orange dye from aqueous media. The sorption of Vat orange dye by FeNPs was observed to be dependent on contact time, temperature, initial adsorbate concentration, adsorbent dosage and pH. Similarly, removal efficiency of the dye molecules increased with a rise in contact time and temperature but fell with an increase in pH. The results suggest that the Freundlich adsorption model is a better fit for the experimental data than the Langmuir isotherm. Based on the data from the study, FeNPs-TE appeared to be the more efficient biosynthesized nanomaterial employed in the degradation of dye molecules. This is in agreement with evidence from the TEM images of nanomaterials obtained.

Results from the experiements suggest that, the biosynthesized iron nanomaterials present a potent and environmentally benign alternative material for the removal of dyes from wastewater.

CHAPTER FIVE

5.0. Conclusions and perspectives

5.1. Conclusions

The role of FeNPs clean-up technology as an alternative to conventional environmental remediation methods is not in doubt considering its widespread use in recent times, as reported in the literature. The inherent properties of FeNPs such as small size, larger surface area, and high reactivity have promoted their use in the remediation of several environmental contaminants. More importantly, understanding of their reactivity with target contaminants and the factors that affect their makeup are integral in the assessment of their effectiveness as good remediating candidates. This, therefore, provided the basis for the current study where green iron nanomaterials were synthesized and utilized in the degradation of an aqueous solution of Vat orange dye. Major findings from the study suggest the production of highly reactive zero state iron nanomaterials with good promise towards the degradation of Vat dyes. The experiments carried out clearly demonstrate the role played by various conditions including pH, temperature, contact time and relative dosages on the degradation of synthetic dyes.

The sorption and removal of the Vat orange dye by the ‘as synthesized’ FeNPs were directly proportional to all the factors studied except pH and initial dye concentration.

Adsorption studies carried out in the present work failed to conclusively attribute the mode of adsorption of the dye molecules by the nanoparticles. However, the Freundlich isotherm model emerged as a better fit for the experimental data obtained.

5.2. Perspectives

Over the last couple of years, green synthesized iron nanoparticles (FeNPs) clean-up technology has been widely embraced as a sustainable and environmentally benign alternative for environmental remediation. Currently, research outcome on the fate and toxicity of FeNPs, post-application is being sought, even though the contrast in their effectiveness to remediate a myriad of environmental contaminants cannot be overelaborated.

The present results on FeNPs clean-up of Vat orange dye in an aqueous solution are based on laboratory studies by simulation of field conditions, and give a good indication of the effectiveness of iron nanomaterials as potential environmental remediating agents. However, field conditions may not be adequately simulated in the laboratory; hence, field experiments may be essential in the provision of more realistic and concrete knowledge of dye degradation by biosynthesized iron nanomaterials.

REFERENCES

Afsheen, S., Tahir, M. B., Iqbal, T., Liaqat, A., & Abrar, M. (2018). Green synthesis and characterization of novel iron particles by using different extracts. *Journal of Alloys and Compounds, 732*, 935-944. doi:10.1016/j.jallcom.2017.10.137

Amendola, V., Meneghetti, M., Granozzi, G., Agnoli, S., Polizzi, S., Riello, P., . . . Sangregorio, C. (2011). Top-down synthesis of multifunctional iron oxide nanoparticles for macrophage labelling and manipulation. *Journal of Materials Chemistry*, 21(11), 3803. doi:10.1039/c0jm03863f

An, K., Somorjai, G.A., (2012). Size and shape control of metal nanoparticles for reaction selectivity in catalysis, *ChemCatChem 4* 1512–1524.

Ashamed, M. I. N. (2014). Ecotoxicity concert of nano zero-valent iron particles- a review. *Journal of Critical Reviews*.

Azuma, R., Nakamichi, S., Kimura, J., Yano, H., Kawasaki, H., Suzuki, T., . . . Obora, Y. (2018). Solution Synthesis of N,N-Dimethylformamide-Stabilized Iron-Oxide Nanoparticles as an Efficient and Recyclable Catalyst for Alkene Hydrosilylation. *ChemCatChem, 10*(11), 2378-2382. doi:10.1002/cctc.201800161.

Bashair H Al Kinani, L. A. A. (2017). Biosynthesis of Cupper Nanoparticles Using Coriandrum sativum L. Ethanolic Extract. *Der Pharma Chemica*.

Bishnoi, S., Kumar, A., & Selvaraj, R. (2018). Facile synthesis of magnetic iron oxide nanoparticles using inedible Cynometra ramiflora fruit extract waste and their photocatalytic degradation of methylene blue dye. *Materials Research Bulletin, 97*, 121-127. doi:10.1016/j.materresbull.2017.08.040

Brown, H.C., Brown, C.A., (1962). A simple preparation of highly active platinum metal catalysts for catalytic hydrogenation. *J. Am. Chem. Soc. 84 (8)*, 1494-1495.

Calderon, B., & Fullana, A. (2015). Heavy metal release due to aging effect during zero valent iron nanoparticles remediation. *Water Res, 83*, 1-9. doi:10.1016/j.watres.2015.06.004

Cao, D., Jin, X., Gan, L., Wang, T., & Chen, Z. (2016). Removal of phosphate using iron oxide nanoparticles synthesized by eucalyptus leaf extract in the presence of CTAB surfactant. *Chemosphere, 159*, 23-31. doi:10.1016/j.chemosphere.2016.05.080

Carroll, D.O., Sleep, B., Krol, M., Boparai, H., Kocur, C., (2013). Nanoscale zero valent iron and bimetallic particles for contaminated site remediation. *Adv. Water Resour*. 51, 104–122.

Chekli, L., Bayatsarmadi, B., Sekine, R., Sarkar, B., Shen, A. M., Scheckel, K. G., . . . Donner, E. (2016). Analytical characterisation of nanoscale zero-valent iron: A methodological review. *Anal Chim Acta, 903*, 13-35. doi:10.1016/j.aca.2015.10.040

Chen, Z. X., Jin, X. Y., Chen, Z., Megharaj, M., & Naidu, R. (2011). Removal of methyl orange from aqueous solution using bentonite-supported nanoscale zero-valent iron. *J Colloid Interface Sci, 363*(2), 601-607. doi:10.1016/j.jcis.2011.07.057

Chien, C.C., Inyang, H.I., Everett, L.G., (2005). Barrier Systems for Environmental Contaminant Containment and Treatment. CRC Press, Boca Raton, FL, USA.

Chu, H., Dong, B., Zhang, Y., Zhou, X., & Yu, Z. (2012). Pollutant removal mechanisms in a bio-diatomite dynamic membrane reactor for micro-polluted surface water purification. Desalination, 293, 38-45. doi:10.1016/j.desal.2012.02.021

Comba, S., Dalmazzo, D., Santagata, E., Sethi, R., (2011). Rheological characterization of xanthan suspensions of nanoscale iron for injection in porous media. *J. Hazard. Mater. 185* (2), 598-605.

Corias, A., Ennas, G., Licheri, G., Marongiu, G., Paschina, G., (1990). Amorphous metallic powders prepared by chemical-reduction of metal-ions with potassium borohydride in aqueous-solution. *Chem. Mater. 2* (4), 363-366.

Crane, R. A., Dickinson, M., & Scott, T. B. (2015). Nanoscale zero-valent iron particles for the remediation of plutonium and uranium contaminated solutions. *Chemical Engineering Journal, 262*, 319-325. doi:10.1016/j.cej.2014.09.084

Devatha, C. P., Thalla, A. K., & Katte, S. Y. (2016). Green synthesis of iron nanoparticles using different leaf extracts for treatment of domestic waste water. *Journal of Cleaner Production, 139*, 1425-1435. doi:10.1016/j.jclepro.2016.09.019

Dey S, Bhattacharjee S, Bose RS, Ghosh CK. Room temperature synthesis of hydrated nickel (III) oxide and study of its effect on Cr(VI) ions removal and bacterial culture. *Appl Phys A Mater Sci Process*. 2015;119:1343–54.

Druzhinina, T. S., Herzer, N., Hoeppener, S., & Schubert, U. S. (2011). Formation of iron oxide particles by reduction with hydrazine. *Chemphyschem, 12*(4), 781-784. doi:10.1002/cphc.201000759

Fu, X., Cai, J., Zhang, X., Li, W. D., Ge, H., & Hu, Y. (2018). Top-down fabrication of shape-controlled, monodisperse nanoparticles for biomedical applications. Adv Drug Deliv Rev, 132, 169-187. doi:10.1016/j.addr.2018.07.006

Gautam, A., Rawat, S., Verma, L., Singh, J., Sikarwar, S., Yadav, B. C., & Kalamdhad, A. S. (2018). Green synthesis of iron nanoparticle from extract of waste tea: An application for phenol red removal from aqueous solution. Environmental Nanotechnology, Monitoring & Management, 10, 377-387. doi:10.1016/j.enmm.2018.08.003

Genuino, H. C., Mazrui, N., Seraji, M. S., Luo, Z., & Hoag, G. E. (2013). Green Synthesis of Iron Nanomaterials for Oxidative Catalysis of Organic Environmental Pollutants. 41-61. doi:10.1016/b978-0-444-53870-3.00003-4

Gillham RW., (1993). Cleaning halogenated contaminants from groundwater: *U.S. Patent No.* 5, 266, 213. 1993; 11-30.

Giraldo, L., Erto, A., & Moreno-Piraján, J. C. (2013). Magnetite nanoparticles for removal of heavy metals from aqueous solutions: synthesis and characterization. *Adsorption, 19*(2-4), 465-474. doi:10.1007/s10450-012-9468-1

Glavee, G.N., Klabunde, K.J., Sorensen, C.M., Hadjipanayis, G.C., (1995). Chemistry of borohydride reduction of iron(II) and iron(III) ions in aqueous and nonaqueous media-formation of nanoscale Fe, Feb, and Fe2B powders. *Inorg. Chem. 34* (1), 28-35.

Gould, J., (1982). The kinetics of hexavalent chromium reduction by metallic iron. *Water Res. 16* (6), 871-877.

Guan, X., Sun, Y., Qin, H., Li, J., Lo, I.M., He, D., Dong, H., (2015). The limitations of applying zero-valent iron technology in contaminants sequestration and the corresponding countermeasures: the development in zero-valent iron technology in the last two decades (1994-2014). *Water Res. 75*, 224-248.

Hatzinger, P.B., (2005). Perchlorate biodegradation for water treatment. *Environ. Sci. Technol. 39* (11), 239A-247A.

Happi Emaga, T., Andrianaivo, R. H., Wathelet, B., Tchango, J. T., & Paquot, M. (2007). Effects of the stage of maturation and varieties on the chemical composition of banana and plantain peels. *Food Chemistry, 103*(2), 590-600. doi:10.1016/j.foodchem.2006.09.006

He, F., Zhao, D., (2005). Preparation and characterization of a new class of starchstabilized bimetallic nanoparticles for degradation of chlorinated hydrocarbons in water. *Environ. Sci. Technol. 39* (9), 3314-3320.

He, F., Zhao, D., (2007). Manipulating the size and dispersibility of zerovalent iron nanoparticles by use of carboxymethyl cellulose stabilizers. *Environ. Sci. Technol. 41* (17), 6216-6221.

He, N., Li, P., Zhou, Y., Ren, W., Fan, S., & Verkhozina, V. A. (2009). Catalytic dechlorination of polychlorinated biphenyls in soil by palladium-iron bimetallic catalyst. *J Hazard Mater, 164*(1), 126-132. doi:10.1016/j.jhazmat.2008.07.149

Holkar, C. R., Jadhav, A. J., Pinjari, D. V., Mahamuni, N. M., & Pandit, A. B. (2016). A critical review on textile wastewater treatments: Possible approaches. *J Environ Manage, 182*, 351-366. doi:10.1016/j.jenvman.2016.07.090

Jin, X., Liu, Y., Tan, J., Owens, G., & Chen, Z. (2018). Removal of Cr(VI) from aqueous solutions via reduction and absorption by green synthesized iron nanoparticles. *Journal of Cleaner Production, 176*, 929-936. doi:10.1016/j.jclepro.2017.12.026

Johnson, R.L., Nurmi, J.T., O'Brien Johnson, G.S., Fan, D., O'Brien Johnson, R.L., Shi, Z., et al., (2013). Field-scale transport and transformation of carboxymethylcellulose-stabilized nano zero-valent iron. *Environ. Sci. Technol*. 47 (3), 1573–1580.

Karn, B., Kuiken, T., & Otto, M. (2009). Nanotechnology and in Situ Remediation: A Review of the Benefits and Potential Risks. *Environmental Health Perspectives, 117*(12), 1823-1831.

Kassaee, M. Z., Motamedi, E., Mikhak, A., & Rahnemaie, R. (2011). Nitrate removal from water using iron nanoparticles produced by arc discharge vs. reduction. *Chemical Engineering Journal, 166*(2), 490-495. doi:10.1016/j.cej.2010.10.077.

Katata-Seru, L., Moremedi, T., Aremu, O. S., & Bahadur, I. (2017). Green synthesis of iron nanoparticles using Moringa oleifera extracts and their applications: Removal of nitrate from water and antibacterial activity against Escherichia coli. *Journal of Molecular Liquids*. doi:10.1016/j.molliq.2017.11.093

keane, e. (2009). Fate, Transport, and Toxicity of Nanoscale Zero-Valent Iron (nZVI) Used During Superfund Remediation. *U.S. Environmental Protection Agency Office of Solid Waste and Emergency Response Office of Superfund Remediation and Technology Innovation*.

Kharissova, O. V., Dias, H. V. R., Kharisov, B. I., Pérez, B. O., & Pérez, V. M. J. (2013). The greener synthesis of nanoparticles. *Trends in Biotechnology, 31*(4), 240-248. doi:10.1016/j.tibtech.2013.01.003

Kisiel,W., Barszcz, B., (1999). Further sesquiterpenoids and phenolics from *Taraxacum officinale*. *Fitoterapia 71* (2000), 269-273.

Kostyukova, D., & Chung, Y. H. (2016). Synthesis of Iron Oxide Nanoparticles Using Isobutanol. *Journal of Nanomaterials, 2016*, 1-9. doi:10.1155/2016/4982675

Kreyling, W. G., Semmler-Behnke, M., & Möller, W. (2006). Health implications of nanoparticles. *Journal of Nanoparticle Research, 8*(5), 543-562. doi:10.1007/s11051-005-9068-z

Ksv, G. (2017). Green Synthesis of Iron Nanoparticles Using Green Tea leaves Extract. *Journal of Nanomedicine & Biotherapeutic Discovery*, 07(01). doi:10.4172/2155-983x.1000151

Kumar, A., & Dixit, C. K. (2017). Methods for characterization of nanoparticles. 43-58. doi:10.1016/b978-0-08-100557-6.00003-1

Laurent, S., Forge, D., Port, M., Roch, A., Robic, C., Vander Elst, L., Muller, R.N., (2008). Magnetic iron oxide nanoparticles: synthesis, stabilization, vectorization, physicochemical characterizations, and biological applications. *Chem. Rev. 108* (6), 2064-2110.

Li H, Zhou Q, Wu Y, F J, Wang T and Jiang G. 2009. Effects of waterborne nano-iron on medaka (Oryzias latipes): Antioxidant enzymatic activity, lipid peroxidation and histopathology. Ecotoxicol Environ Saf. 72(3):684-692.

Li, S., Yan, W., Zhang, W.X., (2009). Solvent-free production of nanoscale zero-valent iron (nZVI) with precision milling. *Green Chem. 11* (10), 1618-1626.

Li, X.-q., Elliott, D. W., & Zhang, W.-x. (2006). Zero-valent iron nanoparticles for abatement of environmental pollutants: materials and engineering aspects. *Critical reviews in solid state and materials sciences*, *31*(4), 111-122.

Liu, Y., Lowry, G.V., (2006). Effect of particle age (Fe^0 content) and solution pH on NZVI reactivity: H_2 evolution and TCE dechlorination. *Environ. Sci. Technol.* 40 (19), 6085–6090.

Machado, S., Pacheco, J. G., Nouws, H. P., Albergaria, J. T., & Delerue-Matos, C. (2015). Characterization of green zero-valent iron nanoparticles produced with tree leaf extracts. *Sci Total Environ, 533*, 76-81. doi:10.1016/j.scitotenv.2015.06.091

Murgueitio, E., & Debut, A. (2016). Synthesis of Iron Nanoparticles using Extracts of Native Fruits of Ecuador, as Capuli (Prunus serotina) and MortiÃƒÂ±o (Vaccinium floribundum). *Biology and Medicine, 08*(03). doi:10.4172/0974-8369.1000282

Narayanan, K. B., & Sakthivel, N. (2010). Biological synthesis of metal nanoparticles by microbes. *Adv Colloid Interface Sci, 156*(1-2), 1-13. doi:10.1016/j.cis.2010.02.001

Nabiyouni, G., Julaee, M., Ghanbari, D., Aliabadi, P.C., Safaie, N., (2015). Room temperature synthesis and magnetic property studies of Fe^3O_4 nanoparticles prepared by a simple precipitation method. *J. Ind. Eng. Chem*. 21 (2015) 599–603.

O'Hannesin, S.F., Gillham, R.W., (1992). A permeable reaction wall for in situ degradation of halogenated organic compounds. In: The 45th Canadian Geotechnical Society Conference, 25-28 October 1992, Toronto, Ontario, Canada.

Ohemeng, P. O., Dankyi, E., Darko, S., Yaya, A., Salifu, A. A., Ahenkorah, C., & Apalangya, V. A. (2020). Iron and silver nanostructures: Biosynthesis, characterization and their catalytic properties. Nano-Structures&Nano-Objects,22100453. doi:10.1016/j.nanoso.2020.100453

Pavan Kumar Gautam, A. S., Krishna Misra, Amaresh Kumar Sahoo,Sintu Kumar Samanta. (2019). Synthesis and applications of biogenic nanomaterials in drinking and wastewater treatment.*Journal of Environmental Management*, *231*, 734–748. doi:10.1016/j.jenvman.2018.10.104

Phenrat, T., Saleh, N., Sirk, K., Tilton, R.D., Lowry, G.V., (2006). Aggregation and sedimentation of aqueous nanoscale zerovalent iron dispersions. *Environ. Sci. Technol.* 41 (1), 284–290

Phenrat, T., Thongboot, T., & Lowry, G. V. (2016). Electromagnetic Induction of Zerovalent Iron (ZVI) Powder and Nanoscale Zerovalent Iron (nZVI) Particles Enhances Dechlorination of Trichloroethylene in Contaminated Groundwater and Soil: Proof of Concept. *Environ Sci Technol*, *50*(2), 872-880. doi:10.1021/acs.est.5b04485

Radini, I. A., Hasan, N., Malik, M. A., & Khan, Z. (2018). Biosynthesis of iron nanoparticles using Trigonella foenum-graecum seed extract for photocatalytic methyl orange dye degradation and antibacterial applications. *J Photochem Photobiol B*, *183*, 154-163. doi:10.1016/j.jphotobiol.2018.04.014

Rebitanim, N. Z., Wan Ab Karim Ghani, W. A., Rebitanim, N. A., & Amran Mohd Salleh, M. (2013). Potential applications of wastes from energy generation particularly biochar in Malaysia. *Renewable and Sustainable Energy Reviews, 21*, 694-702. doi:10.1016/j.rser.2012.12.051

Saif, S., Tahir, A., & Chen, Y. (2016). Green Synthesis of Iron Nanoparticles and Their Environmental Applications and Implications. *Nanomaterials (Basel), 6*(11). doi:10.3390/nano6110209

Sangami, S., & Manu, B. (2017). Synthesis of Green Iron Nanoparticles using Laterite and their application as a Fenton-like catalyst for the degradation of herbicide Ametryn in water. Schlesinger, H.I., Brown, H.C., Finholt, A.E., Gilbreath, J.R., Hoekstra, H.R., Hyde, E.K., ((1953). New developments in the chemistry of diborane and of the borohydrides .9. Sodium borohydride, its hydrolysis and its use as a reducing agent and in the generation of hydrogen. *J. Am. Chem. Soc. 75* (1), 215-219.

Schrick, B., Hydutsky, B.W., Blough, J.L., Mallouk, T.E., (2004). Delivery vehicles for zerovalent metal nanoparticles in soil and groundwater. *Chem. Mater. 16* (11), 2187-2193.

Senthil Kumar, P., Varjani, S. J., & Suganya, S. (2017). Treatment of dye wastewater using an ultrasonic aided nanoparticle stacked activated carbon: Kinetic and isotherm modelling. *Bioresour Technol, 250*, 716-722. doi:10.1016/j.biortech.2017.11.097

Senzaki, T., (1991). Removal of chlorinated organic compounds from wastewater by reduction process: III. Treatment of trichloroethylene with iron powder. *Kogyo Yosui 391*, 29-35.

Senzaki, T., Kumangai, Y., (1988a). Removal of chlorinated organic compounds from wastewater by reduction process: treatment of 1, 1, 2, 2-tetrachloroethane with iron powder. *Kogyo Yosui 357* (2), 2-7.

Senzaki, T., Kumangai, Y., (1988b). Removal of chlorinated organic compounds from wastewater by reduction process: II. Treatment of tetrachloroethane with iron powder. *Kogyo Yosui 369*, 19-25.

Shah, A., Hussain, I., & Murtaza, G. (2018). Chemical synthesis and characterization of chitosan/silver nanocomposites films and their potential antibacterial activity. *Int J Biol Macromol, 116*, 520-529. doi:10.1016/j.ijbiomac.2018.05.057

Shanker, U., Jassal, V., & Rani, M. (2017). Green synthesis of iron hexacyanoferrate nanoparticles: Potential candidate for the degradation of toxic PAHs. *Journal of Environmental Chemical Engineering, 5*(4), 4108-4120. doi:10.1016/j.jece.2017.07.042

Shen, Y. F., Tang, J., Nie, Z. H., Wang, Y. D., Ren, Y., & Zuo, L. (2009). Preparation and application of magnetic Fe_3O_4 nanoparticles for wastewater purification. Separation and Purification Technology, 68(3), 312-319. doi:10.1016/j.seppur.2009.05.020

Simin Arabi, M. R. S. M. K. (2012). Adsorption kinetics and thermodynamics of vat dye onto nano zero-valent iron. *Indian Journal of Chemical Technology, Vol. 20*, pp. 173-179.

Smuleac, V., Varma, R., Sikdar, S., & Bhattacharyya, D. (2011). Green Synthesis of Fe and Fe/Pd Bimetallic Nanoparticles in Membranes for Reductive Degradation of Chlorinated Organics. *J Memb Sci, 379*(1-2), 131-137. doi:10.1016/j.memsci.2011.05.054

Socas-Rodríguez, B., González-Sálamo, J., Hernández-Borges, J., & Rodríguez-Delgado, M. Á. (2017). Recent applications of nanomaterials in food safety. *TrAC Trends in Analytical Chemistry, 96*, 172-200. doi:10.1016/j.trac.2017.07.002

Sravanthi, K., Ayodhya, D., & Yadgiri Swamy, P. (2018). Green synthesis, characterization of biomaterial-supported zero-valent iron nanoparticles for contaminated water treatment. *Journal of Analytical Science and Technology, 9*(1). doi:10.1186/s40543-017-0134-9

Suh, S. K., Yuet, K., Hwang, D. K., Bong, K. W., Doyle, P. S., & Hatton, T. A. (2012). Synthesis of nonspherical superparamagnetic particles: in situ coprecipitation of magnetic nanoparticles in microgels prepared by stop-flow lithography. J Am Chem Soc, 134(17), 7337-7343. doi:10.1021/ja209245v

Sun, S., Zeng, H., (2002). Size-controlled synthesis of magnetite nanoparticles. *J. Am. Chem. Soc. 124* (28), 8204-8205.

Tian, J. Y., Liang, H., Li, X., You, S. J., Tian, S., & Li, G. B. (2008). Membrane coagulation bioreactor (MCBR) for drinking water treatment. Water Res, 42(14), 3910-3920. doi:10.1016/j.watres.2008.05.025

Tosco, T., Sethi, R., (2010). Transport of non-Newtonian suspensions of highly concentrated micro-and nanoscale iron particles in porous media: a modeling approach. *Environ. Sci. Technol. 44* (23), 9062-9068.

Tourinho, P.S., Van Gestel, C.A.M., Lofts, S., Svendsen, C., Soares, A.M.V.M., Loureiro, S., (2012). Metal-based nanoparticles in soil: fate, behavior, and effects on soil invertebrates. *Environ. Toxicol. Chem.* 31 (8), 1679–1692

Uskokovic, V., Odsinada, R., Djordjevic, S., & Habelitz, S. (2011). Dynamic light scattering and zeta potential of colloidal mixtures of amelogenin and hydroxyapatite in calcium and phosphate rich ionic milieus. *Arch Oral Biol*, *56*(6), 521-532. doi:10.1016/j.archoralbio.2010.11.011

Wang, C.B., Zhang, W.X., (1997). Synthesizing nanoscale iron particles for rapid and complete dechlorination of TCE and PCBs. *Environ. Sci. Technol. 31* (7), 2154-2156.

Wang, T., Lin, J., Chen, Z., Megharaj, M., & Naidu, R. (2014). Green synthesized iron nanoparticles by green tea and eucalyptus leaves extracts used for removal of nitrate in aqueous solution. *Journal of Cleaner Production, 83*, 413-419. doi:10.1016/j.jclepro.2014.07.006

Wang, T., Jin, X., Chen, Z., Megharaj, M., & Naidu, R. (2014). Green synthesis of Fe nanoparticles using eucalyptus leaf extracts for treatment of eutrophic wastewater. Sci Total Environ, 466-467, 210-213. doi:10.1016/j.scitotenv.2013.07.022

Wang, Y., & Ni, Y. (2014). Combination of UV-vis spectroscopy and chemometrics to understand protein-nanomaterial conjugate: a case study on human serum albumin and gold nanoparticles. *Talanta, 119*, 320-330. doi:10.1016/j.talanta.2013.11.026

Wang, Z., Li, X., Gao, M., & Zeng, X. (2012). One-step preparation of amorphous iron nanoparticles by laser ablation. Powder Technology, 215-216, 147-150. doi:10.1016/j.powtec.2011.09.039

Wang, Z., Yu, C., Fang, C., & Mallavarapu, M. (2014). Dye removal using iron–polyphenol complex nanoparticles synthesized by plant leaves. *Environmental Technology & Innovation, 1-2*, 29-34. doi:10.1016/j.eti.2014.08.003

Wanyonyi, W. C., Onyari, J. M., & Shiundu, P. M. (2014). Adsorption of Congo Red Dye from Aqueous Solutions Using Roots of Eichhornia Crassipes: Kinetic and Equilibrium Studies. *Energy Procedia, 50*, 862-869. doi:10.1016/j.egypro.2014.06.105

Weber, E.J., (1996). Iron-mediated reductive transformations: investigation of reaction mechanism. *Environ. Sci. Technol. 30* (2), 716-719.

Weng, X., Jin, X., Lin, J., Naidu, R., & Chen, Z. (2016). Removal of mixed contaminants Cr(VI) and Cu(II) by green synthesized iron based nanoparticles. *Ecological Engineering, 97*, 32-39. doi:10.1016/j.ecoleng.2016.08.003

Xiao-Li Li 1, K. T., Yuan-Yuan Zhang, Xiao-Fang Tu, Ying-Shuo Zhang, Dan-Ye Zhu, Jian-Guo Zhang, Zhao-Jun Wei (2018). Effects of different chemical modifications on the antibacterial activities of polysaccharides sequentially extracted from peony seed dreg. *International Journal of Biological Macromolecules, 116*, 664–675. doi:10.1016/j.ijbiomac.2018.05.082

Xue, W., Huang, D., Zeng, G., Wan, J., Cheng, M., Zhang, C., . . . Li, J. (2018). Performance and toxicity assessment of nanoscale zero valent iron particles in the remediation of contaminated soil: A review. *Chemosphere, 210*, 1145-1156. doi:10.1016/j.chemosphere.2018.07.118

Yan, W., Herzing, A. A., Kiely, C. J., & Zhang, W. X. (2010). Nanoscale zero-valent iron (nZVI): aspects of the core-shell structure and reactions with inorganic species in water. *J Contam Hydrol, 118*(3-4), 96-104. doi:10.1016/j.jconhyd.2010.09.003

Yu, W., Graham, N. J., & Fowler, G. D. (2016). Coagulation and oxidation for controlling ultrafiltration membrane fouling in drinking water treatment: Application of ozone at low dose in submerged membrane tank. Water Res, 95, 1-10. doi:10.1016/j.watres.2016.02.063

Zhang, G. Q., Wu, H. P., Ge, M. Y., Jiang, Q. K., Chen, L. Y., & Yao, J. M. (2007). Ultrasonic-assisted preparation of monodisperse iron oxide nanoparticles. Materials Letters, 61(11-12), 2204-2207. doi:10.1016/j.matlet.2006.08.051

Zhang, R., Su, P., & Yang, Y. (2014). Microwave-assisted preparation of magnetic nanoparticles modified with graphene oxide for the extraction and analysis of phenolic compounds. J Sep Sci, 37(22), 3339-3346. doi:10.1002/jssc.201400767

Zhang, W.X., Wang, C.B., Lien, H.L., (1998). Treatment of chlorinated organic contaminants with nanoscale bimetallic particles. *Catal. Today 40* (4), 387-395.

Zhao, X., Liu, W., Cai, Z., Han, B., Qian, T., & Zhao, D. (2016). An overview of preparation and applications of stabilized zero-valent iron nanoparticles for soil and groundwater remediation. *Water Res, 100*, 245-266. doi:10.1016/j.watres.2016.05.019

Zhu, F., Ma, S., Liu, T., & Deng, X. (2018). Green synthesis of nano zero-valent iron/Cu by green tea to remove hexavalent chromium from groundwater. Journal of Cleaner Production, 174, 184-190. doi:10.1016/j.jclepro.2017